max planck institute
of biochemistry

Method Development for the Identification of the Fusogen Involved in Yeast Mating

Entwicklung von Methoden zur Idenfizierung des in der sexuellen Fortpflanzung von *Saccharomyces cerevisiae* beteiligten Fusogens

Master's Thesis

Zur Erlangung des akademischen Grades

Master of Science Molekulare Biotechnologie

des

Wissenschaftszentrums Weihenstephan für Ernährung, Landnutzung und Umwelt

vorgelegt von

Martin Gerhard Schappert

aus Mainz

angefertigt in dem Department
Zelluläre und molekulare Biophysik
am Max-Planck-Institut für Biochemie
unter Anleitung von
Prof. Petra Schwille

intern betreut von
Prof. Wolfgang Liebl
Lehrstuhl für Mikrobiologie
Technische Universität München

MAX-PLANCK-GESELLSCHAFT

München, den 17. August 2015

Technische Universität München

Acknowledgements

I would like to express my sincere gratitude to my supervisor Dr Matías Hernández for his patience, motivation, immense knowledge and the countless hours he invested in discussions about experiments and eventually this thesis. During my time at the Max Planck Institute he taught me much more than *just* science. He escorted me on my very first clumsy steps, he took me by the hand when I stumbled but most of the time he'd let me roam but keeping an eye out. It was an absolute pleasure to work with him.

I am also immensely thankful to Dr Petra Schwille who provided me with the best research environment one could wish for. Despite her busy schedule she was always able to help me on short notice. It is always inspiring to be near an excellent scientist.

My thanks go to Dr Wolfgang Liebl for volunteering to be my internal supervisor; I *literally* wouldn't have been able to do it without him. I know it is a lot of work for an uncertain profit, but I hope this thesis might be worthwhile.

There are so many other people that I owe this to. I am forever indebted to you. Special thanks for being extra awesome go out to Alois, without whom I would not have lived to see the 2nd year. It is both frustrating and inspiring how good you are.

I don't know where to even begin to thank my family for keeping up with me. Thank you Julia, Anna, Daniel, Papa and Sabine. I know I've been sometimes horrible to you guys; thank you for forgetting.

Papa — thank you once again, because one is not even close to being enough.

Danke für alles Mutti.

I have to thank Conny. Words cannot express how grateful I am knowing and loving you. We both know I could not have done it without you, though you won't admit it. Thank you for being there when I needed you and most of all thank you for being you.

Thanks to all the haters. There, I did it. It's such a douchey thing to say. Somebody remind me to kick this out before printing.

I would like to dedicate this thesis to

Ulla Schappert
1963-2011


11-25
© 1986 Universal Press Syndicate
TRIP!
TA-DAAA !!
WATTERSON

List of Abbreviations

16:0 Biotinyl Cap PE	1,2-dipalmitoyl-*sn*-glycero-3-phosphoethanolamine-N-(cap biotinyl)
CW	Cell wall
CHAPS	3-[(3-cholamidopropyl)dimethylammonio]-1-propanesulfonate
DLS	Dynamic light scattering
HEPES	4-(2-hydroxyethyl)-1-piperazineethanesulfonic acid
PIPES	Piperazine-N,N′-bis(2-ethanesulfonic acid)
PM	Plasma Membrane
POPC	1-Palmitoyl-2-oleoylphosphatidylcholine
POPS	1,2-palmitoyl-oleoyl-*sn*-glycero-3-phosphoserine
SC media	Synthetic Complete Media
SDS	Sodium dodecyl sulfate

Abstract

Das Ziel der vorliegenden Masterarbeit war es, Methoden für einen neuartigen Fusionsassay zu etablieren. Dieser Assay soll dafür verwendet werden, das Fusogen von *Saccharomyces cerevisiae* aufzuklären.

Die Fusion von Membranen ist ein fundamentaler und allgegenwärtiger Prozess in eukaryotischen Zellen, über den wir jedoch bemerkenswert wenig wissen. Bisher am besten erforscht sind intrazelluläre Fusionsprozesse und jene unter Beteiligung viraler Fusogene. Über Zell-Zell Fusion ist mit wenigen Ausnahmen kaum etwas genauer erforscht. *S. cerevisiae*, ein Modellorganismus, dessen Erbgut zu weiten Teilen entschlüsselt ist und an dem beispielhaft viele wichtige Entdeckungen über Zelldifferenzierungsmechanismen gemacht worden sind, bietet sich auch hierfür an. Trotz jahrzehntelanger Forschung ist es jedoch bisher nicht gelungen, dass Fusogen der Hefen zu identifizieren. Dies mag zu großen Teilen daran liegen, dass genetische Studien aufgrund von genetischen Redundanzen und den vielen verschiedenen Phasen, die einer Membranfusion vorausgehen, bisher nicht den gewünschten Erfolg brachten. Bisher sind in der Hefe nur Prm1 und Fig1 als an der Fusion beteiligte Plasmamembran Proteine bekannt. Prm1 wird an der Spitze des „shmoo“, dem Ort der Fusion, angereichert. Δ*prm1* Mutanten verharren in einem Schritt nach der Zellwandremodellierung aber vor der Membranverschmelzung. Allerdings ist die Zellfusion in nur etwa der Hälfte der Zellen defekt, was es als *bona fide* Fusogen disqualifiziert. Die Funktion des Fusogens ist es, die Membranen zusammenzuführen und das Verschmelzen herbeizuführen. Um als Fusogen anerkannt zu werden, muss das Fusogen exprimiert und aktiv am Ort der Membranfusion sein, und es müssen genetische und biochemische *in vitro* Analysen die Notwendigkeit und Hinlänglichkeit für Membranfusionsereignisse zeigen.

Da genetische Studien bisher nicht zur Identifizierung des Fusogens in Hefen geführt haben, verfolgen wir einen anderen, biochemischen Ansatz. MATα-Hefen werden mit **a**-factor stimuliert bevor ihre Zellwand (ZW) enzymatisch verdaut wird, woraus Spheroplasten resultieren. **a**-factor ist ein Pheromon, das von dem gegenteiligen Mating Typ, MAT**a**, sekretiert wird. Als Reaktion darauf werden die Proteine der Fusionsmaschinerie exprimiert und auf der Plasmamembran (PM) präsentiert.

Im zweiten Teil des Assays werden die Plasmamembranproteine des anderen Mating Typs, MAT**a**, in Proteoliposomen rekonstituiert. Auch diesem Schritt geht eine Stimulation mit α-factor voraus — dem Pheromon, das von MATα sekretiert wird. Die MAT**a**-Hefen werden nun mechanisch lysiert und die PM Proteinfraktion wird isoliert und aufgereinigt. Nach der Rekonstitution in markierten Liposomen sollen diese, sofern sie das Fusogen tragen, mit dem Spheroplasten verschmelzen.

Um diesen Fusionsassay umzusetzen, müssen einige Methoden entwickelt und verfeinert werden. Die in dieser vorliegenden Masterarbeit durchgeführten Experimente hatten viele wichtige methodische Meilensteine dieser Assayentwicklung zum Ziel. Der Fusion muss eine Annäherung und ein Anheften voraus gehen. Dieses Anheften, das in Hefen von Agglutininen in der ZW übernommen wird, übernimmt in unserem halb-artifiziellen System eine Biotin-Avidin, bzw. Biotin-Streptavidin Bindung. Um dieses Anheften grundlegend charakterisieren zu können, wird ein Anhefte- oder Attachmentassay etabliert. Mithilfe dieses Attachmentassays können Positiv- und Negativkontrollen für den Fusionsassay definiert werden.

Zuerst musste die Pheromonantwort der von uns genutzten Hefestämmest charakterisiert werden. α-factor ist im Gegensatz zu **a**-factor kommerziell erhältlich und daher führten wir viele

Experimente, die im finalen Fusionsassay mit MATα Zellen durchgeführt werden müssen, zu grundlegenden Charakterisierungszwecken mit MAT**a** Hefen durch. Zusätzlich war bei der verwendeten MAT**a**-Stamm Prm1 mit einem GFP-Tag versehen, um die Pheromonantwort verfolgen zu können. Aber wir untersuchten auch die Pheromonantwort von MATα Zellen mit Hilfe von **a**-factor, der von der Core Facility des Max Planck Institutes für Biochemie nach unseren Vorgaben synthetisiert wurde.

Nachdem wir die optimale Konzentration und Dauer der Pheromonstimulation ermittelt hatten, untersuchten wir den Vorgang des Spheroplastierens, also den Verdau überwiegender Teile der ZW durch eine Glucanase. Unglücklicherweise stellte sich heraus, dass unser Spheroplastierungsprotokoll sich negativ auf die Expression und Polarisation von Prm1 auswirkt, weswegen wir die Reihenfolge überdenken mussten. Von uns unerwartet sind jedoch Spheroplasten ebenso in der Lage, Prm1 in der PM anzureichern und diese Polarisation aufrecht zu erhalten. Für unseren Attachment- und den Fusionassay hieß das, dass wir die Reihenfolge der enzymatischen Verdauung der ZW und der Pheromonstimulation umkehrten: Von nun an wurden Spheroplasten stimuliert statt stimulierte Zellen zu spheroplastieren.

Da Liposomen und Spheroplasten nicht ohne weiteres miteinander wechselwirken, wurden die PM Proteine der Spheroplasten biotinyliert, um später die Liposomen über Avidin oder Streptavidin zu einem Anheften zu bringen. Wir untersuchten, ob das Biotinylieren die Prm1-Expression oder -Polarisation beeinträchtigt, aber dies schien nicht der Fall zu sein. Auch beeinflusste die Pheromonantwort nicht die Aufrechterhaltung der vorausgegangenen Biotinylierung. Durch diese Ergebnisse war eine Hälfte des Attachments- bzw. Fusionsassays methodisch entwickelt.

Um Liposomen mit den gewünschten Eigenschaften zu erhalten, wurden viele verschiedene Ansätze verfolgt. Grundsätzlich war das Ziel, möglichst große Mengen an Liposomen zu produzieren, die einen Farbstoff in selbstlöschender Konzentration eingeschlossen haben. Durch Fusion soll der im Liposom vorhandene Farbstoff im Zytoplasma verteilt werden, welches einen starken Anstieg des Fluoreszenssignals zur Folge hat. Untersucht wurden (1) das Elutionsverhalten der Liposomen in der Gelfiltrationssäule in denen die Liposomen hergestellt bzw. aufgereinigt wurden, (2) die Größe der erhaltenen Liposomen per Dynamic Light Scattering und (3) der Einschluss von Farbstoff mit fluorometrischen Messungen.

Nachdem wir Liposomen mit den gewünschten Spezifikationen herstellen konnten, wurde schlussendlich das Anheften von biotinylierten Liposomen an biotinylierte Spheroplasten unter Verbindung von Avidin (bzw. Streptavidin) untersucht. Hier war z.B. von Interesse, ob es praktikabler ist, das Avidin (bzw. Streptavidin) zu den Liposomen oder zu den Spheroplasten zu geben. Im Rahmen des Attachmentassays ist es vermutlich von Vorteil, das Avidin (bzw. Streptavidin) zuerst mit dem Biotin auf der Oberfläche der Spheroplasten reagieren zu lassen, da überschüssiges Avidin (bzw. Streptavidin) unerwünscht ist und in einer Spheroplasten-suspension leichter wieder entfernt werden kann, z.B. durch (mehrmaliges) Zentrifugieren und Resuspendieren.

Ob Avidin oder Streptavidin für die Assays von Vorteil sind, konnte nicht abschließend geklärt werden: Avidin schien zwar eine höhere Affinität zum oberflächen-biotinylierten Spheroplasten zu besitzen, aber zeigte auch unerwünschte Aggregationsphänomene. Außerdem sollte zumindest theoretisch Streptavidin spezifischer in seiner Bindung zum Biotin sein.

Weiterführende Forschung wird die optimale Avidin-, bzw. Streptavidinkonzentration für den Attachmentassay noch genauer eingrenzen müssen, eventuell unter Zuhilfenahme von weiteren Reinigungsschritten. Als nächstes wird die Fusion in Gegenwart von PEG charakterisiert werden

müssen, als Positivkontrolle für den Fusionsassay. Die PM Proteine müssen in Liposomen rekonstituiert werden; vorläufige Experimente deuten darauf hin, dass dieser Schritt keine unberechenbaren Schwierigkeiten bereit hält. Vor der letztendlichen Etablierung des Fusionsassays müssen noch die Ergebnisse von MAT**a** in MATα Zellen bestätigt werden.

1. Introduction

Fusion of membranes is an essential process in multicellular organisms: it is necessary for such various actions, such as vesicular trafficking, immune reactions, and neurotransmission; and of course sexual reproduction [1]. The very beginning of human life thus originates in a process, which we know remarkably little about: cell-cell fusion [2]. The fertilization of the ovum by the sperm is a dramatic fusion event in which the small male gamete reaches the much larger egg cell after racing its competitors and merges into the newly formed zygote. The sperm's recognition of the egg cell's coat, the zona pellucida, as well as the binding to it and finally the adhesion to the egg plasma membrane is relatively well understood, whereas the fusion itself remains elusive.

In general, we know very little about cell-cell fusion compared to virus-cell fusion and vesicle-cell fusion, of which we have a profound knowledge about the involved mechanisms and fusion machinery. This is largely due to the fact that the different stages of fusion, namely gaining of cellular competence to fuse, membrane recognition and attachment, induction, and activation of the fusion-associated membrane molecule, apposition, and finally lipid bilayers mixing [3], are difficult to investigate directly with genetic studies: mutational defects in fusion does not necessarily hint to a cell fusion protein, or so-called fusogen, but might be a result of processes occurring upstream of the actual fusion event. The function of this fusogen is to bring the membranes closer together and to mediate the mixing of bilayers. Podbilewicz et al. state several gold standards to be met by the potential fusogen to be defined as such: genetics and in vitro biochemical assays must demonstrate the necessity for membrane fusion events; it must be shown that the protein is expressed and active at the fusion site; and expressing the fusogen in heterologous cells has to be sufficient for the induction of cell-cell fusion [4].

1.1. Membrane fusion

Cellular membranes are composed of a lipid bilayer, and in order for these membranes to merge, they have to be remodeled by proteins since the lipid bilayers are stabilized again structural changes by a strong hydrophobic effects [5].

Based on theoretical considerations, the following model is now commonly accepted [6]: firstly the membranes have to establish a contact (**Figure 3.1A**). Fusion proteins have to bring membrane lipid bilayers into close contact of a few nanometers, overcoming the electrostatic repulsion and steric interactions of other membrane proteins. This can be established by either pulling or pushing the membranes toward each other. To minimize the area subject to intermembrane repulsion, it is proposed that local bending can form point like protrusions (**Figure 3.1B**) and thus produce a dehydrated contact between the membranes that decreases the hydrophobic energy of the monolayer rupture. This is presumably facilitated by proteins that induce local dehydration and support membrane fluctuations.

The first intermembraneous lipid connection (**Figure 3.1C**), the hemifusion stalk, is believed to combine deformation of bending, tilt and splay of the monolayers in order to optimize shape and prevent vacuum voids inside the interstices [5]. **Figure 3.1D** depicts the supposed progression via radial expansion of the stalk into a hemifusion diaphragm, a single bilayer formed by the juxtaposition of the inners monolayers. Fusion is completed by a formation of a pore (**Figure 3.1E**). The tendency of lipid bilayers to hemifuse and develop fusion pores heavily depends on lipid composition [5].

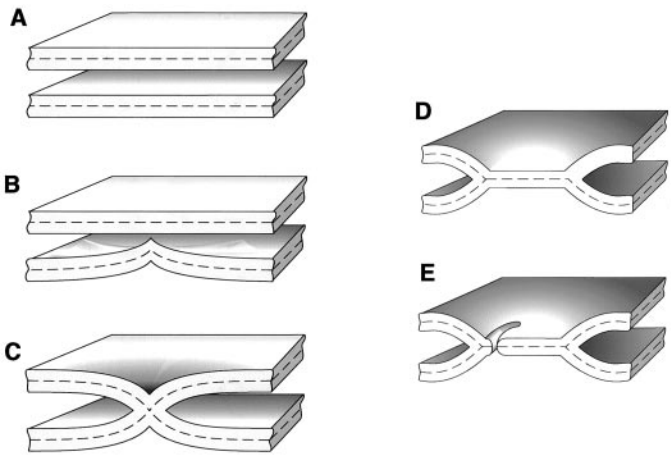

Figure 3.1 Fusion of lipid bilayers. A) Establishment of membrane contact. **B)** Pointlike protrusion at the prefusion stage. **C)** Fusion stalk. **D)** Hemifusion Diaphragm. **E)** Cracklike fusion pore. [5]

It was shown that intracellular compartments undergoing immanent remodeling have high local concentrations of cone-shaped lipids. Moreover, some fusion reactions are believed to be regulated by phospholipase activity [7, 8]. However, experiments on viral and intracellular fusogens reconstituted in proteoliposomes showed that fusogenic lipids are not indispensable [6]. This strongly suggests that alterations in the local lipid composition is not the only way for proteins to promote fusion.

1.1.1. Cell-cell fusion in fertilization

Currently there are only three candidate genes identified that are essential in sperm-egg fusion in mice: Izumo1 on the spermatozoon, its GPI-anchored receptor on the plasma membrane of the oocyte, Juno, and Cd9 (which is also found on the egg cell membrane). Deletion of the corresponding genes results in severely reduced fertility [9,10,11].

Cd9 is a member of the tetraspanin family and is ubiquitously expressed. It is involved in fusion of myoblasts and monocytes, interacting with immunoglobulins, G proteins and other adhesion molecules [12, 13]. Wild type sperm are able to penetrate the zona pellucida of $Cd9^{-/-}$ oocytes, bind to the oolemma but fail to fuse [11]. The function of Cd9 in fusion seems polyvalent: it has been shown that it plays a role in sperm-egg binding [14], in structuring the membrane and in *cis*-interactions with other membrane proteins [15].

Izumo1 functionally only possesses an immunoglobulin domain and lacks any fusogenic peptide domain. Neither of them contains a domain resembling fusogenic peptides in viral fusogens or intracellular vesicular trafficking. Therefore it is plausible that Izumo1 might interact with associated proteins in a multiprotein complex [16].

Juno is highly expressed on unfertilized eggs. The pattern of expression matches to the pattern of Izumo1 binding and treatment with antibody inhibits fusion. Female mice are absolutely infertile while the males remain fertility. Interaction of Izumo1 and Juno seems, though essential and necessary, not to be of fusogenic nature but rather an adhesion step that precedes fusion [10].

Why is it that we know so little about this fundamental process? Sterility as a phenotype of a knock-out has only been demonstrated in male $Izumo1^{-/-}$ and female $Juno^{-/-}$ mice; whereas

subfertile phenotypes might result in sterility when combined, such as in $Cd9^{-/-}/Cd81^{-/-}$ [17]. This redundancy renders genetic studies a challenging endeavor.

However, besides the fusogens involved cell-cell fusion in fertilization, we know of a few more fusogens. Among the best-studied are viral fusogens.

1.1.2. Viral cell fusion

Enveloped viruses, such as the influenza virus and HIV, use transmembrane viral proteins to mediate fusion with host cell membranes. To date, three structurally different types of viral fusion proteins are recognized [18]:

- **Class I** fusion proteins, such as human immunodeficiency virus (HIV) gp41, have a characteristic postfusion conformation with a signature trimer of α-helical hairpins with a central coiled-coil structure.
- **Class II** fusion proteins, such as dengue E glycoprotein, have a structural signature of β-sheets forming an elongated ectodomain that refolds to result in a trimer of hairpins. These proteins lack the central coiled coil.
- **Class III** fusion proteins, such as the rabies virus G glycoprotein, combine structural signatures found in classes I and II.

[19]

Viral fusogens utilize the free energy that is liberated from the vast conformational changes they undergo as they pull the membranes together. **Figure 3.2** presents a schematic sequence of events in viral fusogen-mediated cell membrane fusion. It generally applies to all viral fusion proteins, regardless of class [18].

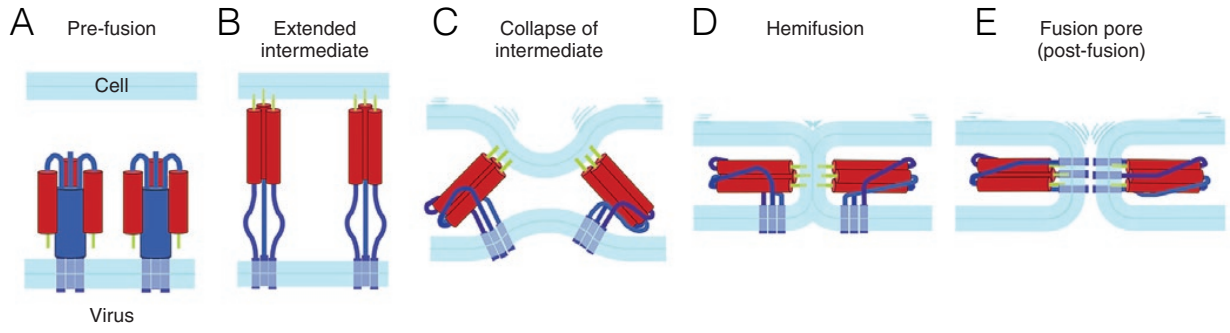

Figure 3.2 Schematic sequence of events in virus-cell membrane fusion. A) In the pre-fusion conformation the fusion peptide or loop is sequestered. **B)** Extension of the fusion peptide or loop projecting into the target membrane. A trimeric cluster forms at the part of the protein that bears the fusion peptide or loop. **C)** Collapsing of the subunits distorts the membrane. **D)** Hemifusion occurs when the two bilayers come into contact and merge into a hemifusion stalk. **E)** The hemifused bilayers open into a fusion pore as the protein refolds into its symmetric post-fusion conformation, effectively preventing the pore from resealing. [18]

All known viral fusion proteins are trimeric in their functional state [18]. There is a C-terminal transmembrane anchor holding the protein in place at the viral membrane and a fusion peptide or loops interacting with the target bilayer. The process is suggested to be initiated by a bridge formation between the two membranes (**Figure 3.2B**). The fusion peptide or loops are

brought together when the extending domains collapse, which results in deformation of the membranes within a small area of close approach (**Figure 3.2C**). An opening of a hemifusion stalk then forms a transient fusion pore. When the protein refolds into a symmetric post-fusion conformation, the pore is irreversibly created and fusion is completed (**Figure 3.2D** and **E**).

1.1.3. SNARE-mediated fusion

Intracellular fusion is mediated by the SNARE (SNAP receptors) family of proteins by the assembly of cognate v- and t-SNAREs on two opposing membranes. The SNARE machinery is highly conserved from yeast and to mammals [20]. There are some who contain lipid anchors, but most are type II membrane proteins with most oriented towards the cytoplasm. All of them contain a SNARE motif consisting of stretches of ~ 60 amino acids with a strong tendency to assemble into a highly conserved coiled coil four-helix bundle structure known as the SNAREpin [20]. Membrane fusion is a result of protein folding during SNAREpin assembly that proceeds in a zipper-like fashion from the membrane distal N-terminus to the C-terminal membrane proximal regions [21, 22].

1.1.4. Cell-cell fusion in *Caenorhabditis elegans*

The model nematode *Caenorhabditis elegans* represents a singular opportunity to study cell-cell fusion. Roughly a third of its 959 somatic cells fuse in a fully reproducible pattern to create multinucleated syncytia [23]. The transmembrane protein *Epithelial Fusion Failure 1* EFF-1 was identified as a candidate fusogen via genetic screening. Subsequent to that finding, homotypic fusion in heterologous cells was shown, demonstrating EFF-1 to be a *bona fide* fusogen [23].
Fusion mediated by EFF-1 follows the same key intermediates as in viral and intracellular fusion, and is structurally homologous to class II viral fusion proteins [24]. It varies from intracellular such as SNARE mediated fusion, which needs different but complementary sets of protein fusogens on the fusing membranes [25]. This need for homotypic organization of fusion *in vivo* provides a better control of the shape and size of the syncytia, preventing fusion with neighboring cells [23].

1.2. Yeast as a model organism

Multicellular organisms frequently comprise various cell types. Mammals for example consist of muscle cells, epithelia, neuronal cells and many others. These specialized cells determine through their specific properties, how tissues, organs and the whole organism function and behave. Scientists try to find more simple models that allow them to obtain more general insights on certain biological events. Findings in those simple models provide the basis to a better understanding of higher organisms.

How do all the different cell types arise from one single cell, the fertilized egg? A well accepted model for cell differentiation is the baker's yeast, *Saccharomyces cerevisiae*, and many fundamental insights learned from yeast apply to humans as well. Aside from the quiescent spores, *S. cerevisiae* exists as one of three cell types: **a** and α are haploid and form the diploid **a**/α cell by mating.

1.2.1. Cell types

Yeast cells are eukaryotic and like plant cells, the plasma membrane is covered by a cell wall (CW) consisting of a network of carbohydrates and proteins. The diploid genome contains some 6000 genes distributed among 16 chromosomes [26]. Haploid yeast cells secrete small peptide pheromones that are cell type-specific and are sensed via cell type-specific receptors: **a** cells produce a pheromone called **a**-factor and respond to α-factor, which is secreted by α cells. α cells in turn are stimulated by **a**-factor. This ensures that **a** and α cells only mate with each other to form diploid **a**/α cells. The receptor on the **a** cell that is stimulated by α-factor is Ste2, while the receptor stimulated by **a**-factor found on α cells is called Ste3 [27].

The haploid cell's initial response to pheromone is to arrest cell division, initiate transcription of specific genes encoding proteins required for the mating process, including the formation of a directed projection towards the source of pheromone, called a „shmoo". This is important because yeast cells cannot move on their own and therefore try to come into contact with each other by growing projections towards each other. The CWs then adhere to each other when the contact is established, and this section of the CW is remodeled by glycosidic enzymes. This allows the plasma membranes (PMs) to establish contact and fuse, forming a single larger cell [28].

a/α cells do not mate, neither with each other nor with **a** or α cells, but are capable of meiosis and sporulation. Under conditions of starvation for carbon and nitrogen, spores are formed because of their enhanced ability to persist these unfavorable conditions. By producing four haploid spores (two of each mating type) in a sac called an ascus, sporulation completes the sexual cycle of yeast. The spores are able to convert into metabolically active yeast cells once the ascus is degraded under favorable conditions. All cell types, in addition to sexual mating and sporulation, are able to proliferate asexually via budding.

1.2.2. Response to the mating pheromone

In order to be able to react to the opposite mating type's pheromone, the yeast cell has to detect the extracellular pheromone and its concentration at a given surface area. As aforementioned **a** cells express the Ste2 receptor that binds α-factor, whereas MATα cells rely on Ste3 to detect **a**-factor. Both belong to the highly conserved family of G protein-coupled receptors with seven trans-membrane domains and binding to the respective mating pheromone elicits interaction with the cytoplasmic G protein [27]. In yeast, the G protein in question is heterotrimeric and is made up of the subunits Gpa1, Ste4, and Ste18 — or, more generally, G_α , G_β, and G_γ. When the receptor binds to a pheromone, it causes the G_α to exchange bound GDP for GTP. This releases the $G_{\beta\gamma}$ complex, which in turn interacts with proteins to continue the signal cascade. The GTP that is bound by G_α is hydrolyzed to GDP so the G protein can reassemble, effectively switching into the „off" state [29]. Continuation of signal transduction can thus only take place when pheromone binds to the receptor again [27].

The unbound $G_{\beta\gamma}$ activates a kinase cascade by recruiting Ste5, a scaffold protein that tethers together Ste11, Ste7 and Fus3. Subsequent phosphorylation, starting with yet another kinase called Ste20, ultimately activates Fus3 that in turn activates transcription factor Ste12 [29]. Ste12 promotes expression of **a**- and α-specific genes (**a**-sgs, α-sgs) and is usually inhibited by Dig1 and Dig2. Fus3 phosphorylates these inhibitors, allowing Ste12 to bind to the promoters of **a**-sgs or α-sgs and activate their transcription. Ste12 also activates a subset of haploid specific

genes (hs-gs) involved in mating by binding to the promoters as a homodimer (see **Figure 3.3**). A basal level of signaling is maintained even without pheromone presence to maintain a baseline of transcription [29].

MAT**a** and MATα cells will lose their sensitivity to pheromone after prolonged exposure through negative feedback mechanisms. This enables them to reenter the cell cycle when mating was not possible up to that point [29].

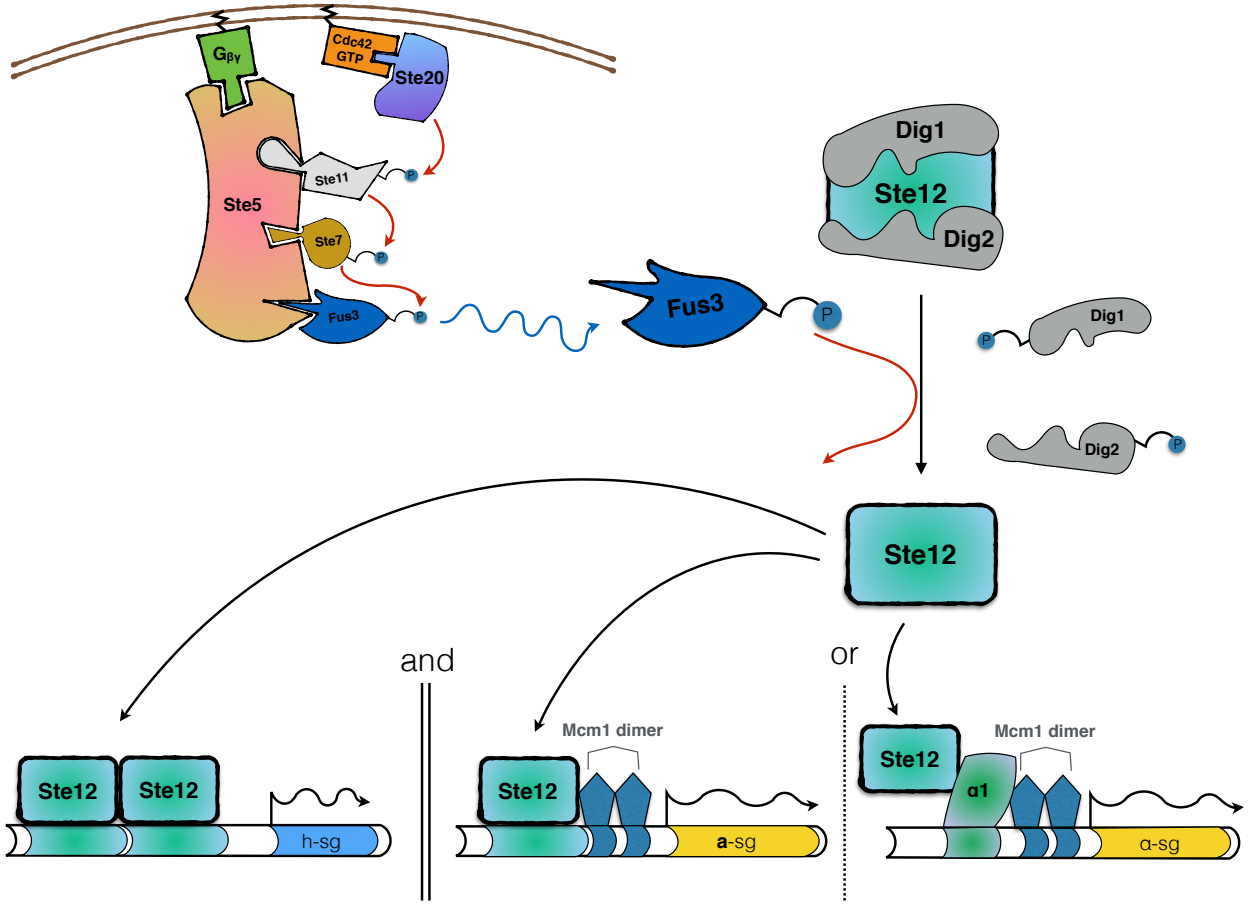

Figure 3.3 Pheromone signal transduction pathway. $G_{\beta\gamma}$ activates the MAP kinase signaling cascade by recruiting the scaffold protein Ste5 to the plasma membrane. Ste11, Ste7 then take part in the kinase cascade, ultimately activating Fus3 that in turn posphorylates Dig1 and Dig2. The transcription factor Ste12 disassociates from its inhibitors and acts binds to the promoters of a-sgs or α-sgs respectively and activate their transcription.

1.2.3. Fig1 and Prm1 in mating yeast

Despite decades of research, genetic studies have not been able to identify the yeast fusogen. Indeed, there are only two PM proteins that have been shown to be directly involved in cell fusion of mating yeast: Prm1 [30] and Fig1 [31]. Δ*prm1* mutants halt just after CW remodeling but prior to membrane fusion, an effect which is enhanced in Δ*fig1* background. In addition Δ*prm1* and Δ*fig1* result in more mating pairs lysing during a failed fusion attempt. However, about half of the mating pairs are able to fuse nevertheless, suggesting both Prm1 and Fig1 are non-essential, accessory components of the fusion machinery [30, 31]. This is also suggested by studies that found that a small amount of Prm1 was enough to promote fusion [28]. Prm1 is also implicated to be involved in cell fusion in *Schizosaccharomyces pombe*, in which it is shown to take part in membrane reorganization [32].

2. Materials and Methods

2.2. Materials

A list of chemicals and suppliers can be found in **Table 2.1** and laboratory equipment in **Table 2.2**. The software used in this thesis is found in **Table 2.3**.

Table 2.1 Chemicals

Chemical	Supplier	Used In
a-factor	Core facility, MPG	Pheromone treatment
α-factor Mating Pheromone	GenScript	**2.10.**, pheromone treatment
CHAPS	Serva	**2.3.4.**
D-Sorbitol	Sigma Life Science	**2.3.2.**, **2.3.3.**, **2.3.4.**, **2.3.5.**, **2.3.6.**, **2.3.7.**
EZ-Link Sulfo-NHS-LC-Biotin	Thermo Scientific	**2.7.**
Glycine	Sigma-Aldrich	**2.7.**
HEPES	biomol	**2.3.4.**, **2.3.5.**, **2.3.6.**, **2.3.7.**
Pierce Avidin	Thermo Scientific	**2.9.**
PIPES	Sigma Life Science	**2.3.2.**, **2.3.3.**
Poly-L-lysine	Sigma Life Science	Passivation of slides
SC Broth / 2% Glucose	Formedium	**2.3.1.**
SDS	Sigma Life Science	**2.7.**, osmotic lysis test
Streptavidin Alexa Fluor 555	Life technologies	**2.9.**
Streptavidin lyophil. saltfree	Serva	**2.11.**
Sulforhodamine B	Sigma Life Science	**2.3.4.**, **2.3.5.**
TRITON X-100	Sigma Life Science	**2.7.**
Zymolyase 100T	USBiological	**2.8.**
Lipids	Avanti	**2.3.8.**

Table 2.2 Laboratory Equipment

Name	Supplier	Category
LSM 510, ConfoCor 3	Carl Zeiss	Confocal Microscope Body
IX50	Olympus	Lightfield Microscope Body
Centrifuge 5804	eppendorf	Table Centrifuge
Centrifuge 5424	eppendorf	Table Centrifuge
BioSpectrometer	eppendorf	Spectrometer
innova 42	New Brunswick Scientific	Incubator
Thermomixer Comfort	eppendorf	Thermomixer
ÄKTApure	GE Health	Chromatograph
HiTrap Desalting (5mL)	GE Health	Size Exclusion Column
Superdex™ Peptide 3.2/300	GE Health	Size Exclusion Column
Superdex™ 200 Increase 5/150 GC	GE Health	Size Exclusion Column
Zetasizer Nano	Malvern	Dynamic Light Scattering Measurement
FP-8500	Jasco	Fluorometer
Laborata 4000, CVC 3000	Heidolph, Vacuubrand	Rotary Evaporator
Slide-A-Lyzer® 3500 MWCO, 0.1-0.5 mL Capacity	Thermo Scientific	Dialysis Cassette
MacBook Pro (Retina, Mid 2012)	Apple	Computer

Table 2.3 Software

Program	Used For
Endnote X6	Literature Management
Fiji	Image Editing
MagicPlot Student	Generating Graphs
Numbers	Generating Tables
Pages	Writing
Keynote	Generating Figures
Excel	Generating Tables
Unicorn 7	ÄKTA Software
ZEN 2009	Confocal Microscope Software
uc480 Viewer	Lightfield Microscope Image Capturing

Table 2.4 Lasers used in confocal microscopy

Wavelength	Excitation of
488 nm	GFP
543 nm	Alexa Fluor 555
543 nm	Sulforhodamine B
633 nm	ATTO 655

2.3. Preparation of Solutions and Media

2.3.1. Synthetic Complete (SC) media

For the preparation of SC media, 28.9 g of SC Broth / 2 % Glucose (Formedium) are dissolved in 1 L of ultra pure water and aliquoted to 250 mL flasks. Sterilization is accomplished by autoclaving.

2.3.2. Spheroplasting Buffer

Spheroplasting Buffer is prepared by dissolving 45.54 g D-Sorbitol and 1.51 g PIPES (both Sigma Life Science) in 250 mL ultra pure water. Adjust to pH 7.5 with NaOH. The resulting 1 M Sorbitol, 20 mM PIPES, pH 7.5 buffer is then sterile filtered through a 0.22 μm filter.

2.3.3. 50/50 Buffer

For 50/50 Buffer preparation, one volume of Spheroplasting Buffer and one volume of SC media are evenly mixed.

2.3.4. Lipid Mix Buffer for preparation of liposomes

Lipid Mix Buffer contains 0.4 M D-Sorbitol, 0.2 M NaCl, 0.1 M Sulforhodamine B, 0.02 M HEPES and 5 % or 2 % (w/v) CHAPS at a pH of 7.5. It is prepared by dissolving 1457 mg D-Sorbitol (Sigma Life Science), 234 mg NaCl (Chemicals VWR BDH Prolabo), 1161 mg Sulforhodamine B (Sigma Life Science) and 95 mg HEPES (biomol) in 20 mL of ultra pure water. Then either 1000 mg or 400 mg of CHAPS (Serva) is added, depending on the desired final concentration. Adjust to pH 7.5 and sterile filtrate through 0.22 μm filter.

2.3.5. Rapid Dilution Buffer

Rapid Dilution Buffer contains the same chemicals and is prepared in a similar manner as the Lipid Mix Buffer, minus the CHAPS. Therefore, Rapid Dilution Buffer contains 0.4 M D-Sorbitol, 0.2 M NaCl, 0.1 M Sulforhodamine B, 0.02 M HEPES at a pH of 7.5. It is prepared by dissolving 1457 mg D-Sorbitol (Sigma Life Science), 234 mg NaCl (Chemicals VWR BDH Prolabo), 1161 mg Sulforhodamine B (Sigma Life Science) and 95 mg HEPES (biomol) in 20 mL of ultra pure water. Adjust to pH 7.5 and sterile filtrate through 0.22 μm filter.

2.3.6. Dialysis Buffer

Dialysis Buffer is isotonic with Lipid Mix Buffer and Rapid Dilution Buffer and contains 0.4 M D-Sorbitol, 0.3 M NaCl and 0.02 M HEPES, pH 7.5. To prepare Dialysis Buffer, dissolve 17,532 g NaCl (Chemicals VWR BDH Prolabo), 72,868 g D-Sorbitol (Sigma Life Science) and 4,766 HEPES (biomol) in 1 L of ultra pure water. Adjust pH to 7.5 and sterile filter through 0.22 μm filter.

2.3.7. Elution Buffer

See **2.3.6. Dialysis Buffer**.

2.3.8. Lipid Mix

2.3.8.1. Preparation of Lipid Mix (small volume)

All lipids were purchased from Avanti Polar Lipids (USA) and stored in chloroform stock solutions sorted at -20 ºC. Mix lipids according to **Tables 2.5** and **2.6** in a brown glass vial, Dry under stream of N_2 and resuspend in Lipid Mix Buffer.

2.3.8.2. Preparation of Lipid Mix (larger volume)

To prepare the Lipid Mix, mix lipids in a round bottom flask according to the **Tables 2.5** and **2.6**. Dry in a rotary evaporator by increasing the vacuum over the course of 1 h to 20 mBar. Once a dried lipid film is obtained, resuspend in appropriate volume of Lipid Mix Buffer. For long-term storage, all lipid mixes were snap frozen in liquid N_2 and kept at -20 ºC.

Table 2.5 Lipid composition as used with second column

Percentage [%]	Lipid	MW [g/mol]	Stock (mg/mL)	Stock (mM)	Amount of lipid [μmole]	Volume to be added to vial [μL]	Weight [mg]
90	POPC	760,08	25	32,89	1,8000	54,7258	1,3681
9,88	POPS	784	10	12,76	0,1976	15,4918	0,1549
0,1	16:0 Biotinyl CAP-PE	1.053	1	0,95	0,0020	2,1053	0,0021
0,02	Atto-655 DSPE	1366	1	0,73	0,0004	0,5464	0,0005
100					2,0000	72,8693	

Final volume of lipid mix (μL)	100,0
Final lipid concentration (mM)	20,0

Table 2.6 Lipid composition as used with third column

Percentage [%]	Lipid	MW [g/mol]	Stock (mg/mL)	Stock (mM)	Amount of lipid [μmole]	Volume to be added to vial [μL]	Weight [mg]
90	POPC	760,08	25	32,89	3,375	102,6108	2,5653
7,95	POPS	784	10	12,76	0,2981	23,3730	0,2337
2	16:0 Biotinyl CAP-PE	1.053	1,25	1,19	0,0750	65,1596	0,0789
0,05	Atto-655 DSPE	1366	1	0,73	0,0019	2,5613	0,0026
100					3,75	191,7047	

Final volume of lipid mix (μL)	150,0
Final lipid concentration (mM)	25,0

2.4. Preparation of liposomes

2.4.1. Rapid Dilution

To prepare liposomes via Rapid Dilution, the CHAPS concentration of the lipid mix is diluted to 0.25% (w/v) or lower. To produce 100 μL of liposome suspension, add 5 μL of Lipid Mix with 95 μL of Rapid Dilution Buffer with thorough mixing. Apply gel filtration chromatography or dialysis to remove excess Sulforhodamine B and detergent.

2.4.2. Dialysis

To prepare liposomes via Dialysis, inject 200 μL of Lipid Mix in a dialysis cassette of a molecular weight cut-off of 3.5 kDa (Thermo Scientific). Dialyze in 500 mL of Dialysis Buffer at 4 °C for 12 h. Exchange for fresh Dialysis Buffer and let again dialyze at 4 °C for 12 h.

Optional: For improved dye encapsulation, Rapid Dilution Buffer can be substituted for Dialysis Buffer.

2.4.3. Gel Filtration

Apply Lipid Mix directly to chromatography system.

2.5. ÄKTApure Methods

Table 2.7 ÄKTApure method HiTrap Desalting (5mL)

Parameter	Value
System flow	0.500 mL/min
Empty loop with	0.150 mL
Elute with	2.20 vol
UV1	280 nm
Fractionation volume	0.500 mL
Total Volume approx.	11.21 mL
Loop volume used	0.100 mL

Table 2.8 ÄKTApure method Superdex™ Peptide 3.2/300

Parameter	Value
System flow	0.150 mL/min
Empty loop with	0.250 mL
Elute with	1.32 CV
Delay fractionation	0.18 CV
UV1	280 nm
UV2	565 nm
Fractionation volume	0.100 mL
Total Volume approx.	3.87 mL
Loop volume used	0.200 mL

Table 2.9 ÄKTApure method Superdex™ 200 increase 5/150 GC

Parameter	Value
System flow	0.250 mL/min
Empty loop with	0.170 mL
Elute with	1.79 CV
Delay fractionation	0.21 CV
UV1	280 nm
UV2	565 nm
Fractionation volume	0.100 mL
Total Volume approx.	6.06 mL
Loop volume used	0.150 mL

2.6. Size analysis of liposomes

To assess the size of the produced liposomes, examine the liposomes via dynamic light scattering (DLS) in a Malvern Zetasizer nano. The Zetasizer determines the size of particles by measuring the diffusion of the particles moving under Brownian motion [33]. Light scattering fluctuations and recording of the auto-correlation function was performed using the manufacturer's acquisition software. Each sample was equilibrated to 25 °C for 120 s. One measurement consisted of 5 readings, and each sample was measured three times.

2.7. Encapsulation test

To analyze liposomal encapsulation of Sulforhodamine B, add 25 μL of liposome suspension to 225 μL of Elution Buffer. Measure basal fluorescence in a fluorometer. Then add 2.5 μL of 20% SDS to the sample and measure increase in fluorescence. The parameters for the measurement can be found in **Table 2.10.**.
Optional: Triton X-100 can be substituted for SDS.

Table 2.10 Parameters used for encapsulation test with Jasco FP-8500

Parameter	Value
Photometric mode	Em intensity
Ex bandwidth	1 nm
Em bandwidth	10 nm
Response	1 s
Sensitivity	High
Data intervall	5 s
Ex wavelength	565 nm
Em wavelength	586 nm
Intensity modification	off
Blank correction	off
Auto gain	off
Light source	Xe Lamp
Filter	Use

2.8. Preparation of spheroplasts

Start an overnight pre-culture two days before and incubate MATα cells in 2 mL of synthetic complete (SC) media at 30 °C. Use overnight pre-culture (200 uL) to inoculate two 10 mL of SC media in separate 100 mL flasks. Grow again overnight at 30 °C.

At the next morning check the OD600. Culture should be between 0.9 – 1.4. If not, dilute with SC and incubate for 2 h at 30 °C. Transfer both 10 mL cultures to separate plastic 15 mL Falcon tubes and spin down at

2500 rcf for 3 min. Remove supernatant and resuspend both pellets with Spheroplasting Buffer and spin at 2500 rcf for 3 min. Repeat the previous step to wash cells once more.

Weigh Zymolyase 100T (1 mg) into two eppendorf tubes of 2 mL. Resuspend the pellet of cells with 2 mL of Spheroplasting Buffer and transfer suspension to the tube containing Zymolyase 100T. Add 10 uL of 0.2 M phenylmethanesulfonylfluoride (PMSF, ##) and mix well with a pipette. Incubate tube in a thermomixer at 35 °C without mixing for 30 minutes. After 15 minutes, very gently mix reaction with a pipette. Spin down tubes containing spheroplasts at 1000 rcf for 2 min. Remove supernatant, wash by resuspending pellet in 2 mL Spheroplasting Buffer. Spin down again and repeat washing twice. After the last centrifugation, resuspend in 1 mL of Spheroplasting Buffer.

2.9. Biotinylation of spheroplasts

Biotinylation of surface proteins of spheroplasts was performed with EZ-Link Sulfo-NHS-LC-Biotin following the manufacturer's instructions (Thermo Scientific). The underlying chemistry is based on a spontaneous reaction of the N-hydroxysuccinimide (NHS) with amines to form an amide bond. Weigh 3 mg of EZ-Link Sulfo-NHS-LC-Biotin in a 1.5 mL eppendorf tube. Transfer 1mL of spheroplast suspension (as prepared in **2.8.**) to the tube containing EZ-Link Sulfo-NHS-LC-Biotin and mix gently with a pipette. Leave tube at room temperature for 30 min with mixing every 5-10 min with a pipette. While waiting, weigh 7.5 mg of glycine (Sigma-Aldrich) in a separate eppendorf tube. Spin down tube at 1000 rcf for 2 min, resuspend in 1 mL of Spheroplasting Buffer and transfer suspension to the tube containing glycine (equals 0.1 M). Centrifuge at 1000 rcf for 2 min and resuspend in 1 mL of Spheroplasting Buffer.

Optional: To check for biotinylation, apply 2.5 μL of 1 mg/mL streptavidin Alexa Fluor 555 (Life Technologies) to 100 μL of spheroplast suspension. Mix gently and leave at room temperature for 30 min with only occasional mixing with a pipette. Assess biotinylation efficiency via confocal microscopy.

2.10. Pheromone treatment of MATa spheroplasts

Spin down spheroplasts that were prepared like described in **2.8.**, or **2.9.** if you want to work with non-biotinylated spheroplasts, and resuspend in the same volume of 50/50 Buffer. Add 0.5 μL of 1 mg/mL α-factor per 100 μL of MAT**a** spheroplasts, equalling ~ 3 x 10^7 spheroplasts. Incubate tube in a thermomixer at 30 °C for 3 h with occasional mixing with a pipette. Centrifuge at 1000 rcf for 2 min and resuspend in Spheroplasting Buffer (skip this if you continue with **2.11.**).

2.11. (Strept-)avidin addition to biotinylated spheroplasts

Prepare a 1mg/mL solution of Streptavidin e (Serva) or Pierce Avidin (Thermo Scientific) in Spheroplasting Buffer. Use spheroplast suspension that was prepared as described in **2.9.**, or **2.10.** respectively, depending on whether you want to work with pheromone-treated spheroplasts. Spin down at 1000 rcf for 2 min. Resuspend spheroplasts in the respective amount of Spheroplasting Buffer containing (strept-)avidin and add Spheroplasting Buffer to a total volume equal to your start volume. Leave tube at room temperature for 30 min with gentle mixing with a pipette every 5-10 min. Centrifuge at 1000 rcf for 2 min and resuspend in Spheroplasting Buffer. Repeat the last step at least once.

3. Results

The goal of this Master's thesis is to develop an assay to investigate the biochemical interactions which are relevant for fusion and which can lead to the identification of the fusogen. In particular, we will utilize proteoliposomes and spheroplasts to bypass the CW. Previous studies with yeast have shown that the removal of the CW impairs fusion between cells of the opposite mating type [34, 35]. However, to be able to distinguish any fusogenic activity from upstream events, it would be advantageous to simplify the reaction to uncouple fusion from processes taking place prior to it. Indeed, this inability to clearly dissect fusion from upstream events has been a major problem for genetic studies focusing on the fusogen of *S. cerevisiae* and has contributed to the fact that it has not been found yet. Until now, only Prm1 has directly been implicated in fusion as shown by the observation that *prm1* knock-outs halt the fusion process after CW remodelling, with the two PMs being in contact but remaining unmerged. However, it is only a partial defect with about half of the mating pairs still fusing, suggesting the existence of a yet-to-be identified fusogen [30].

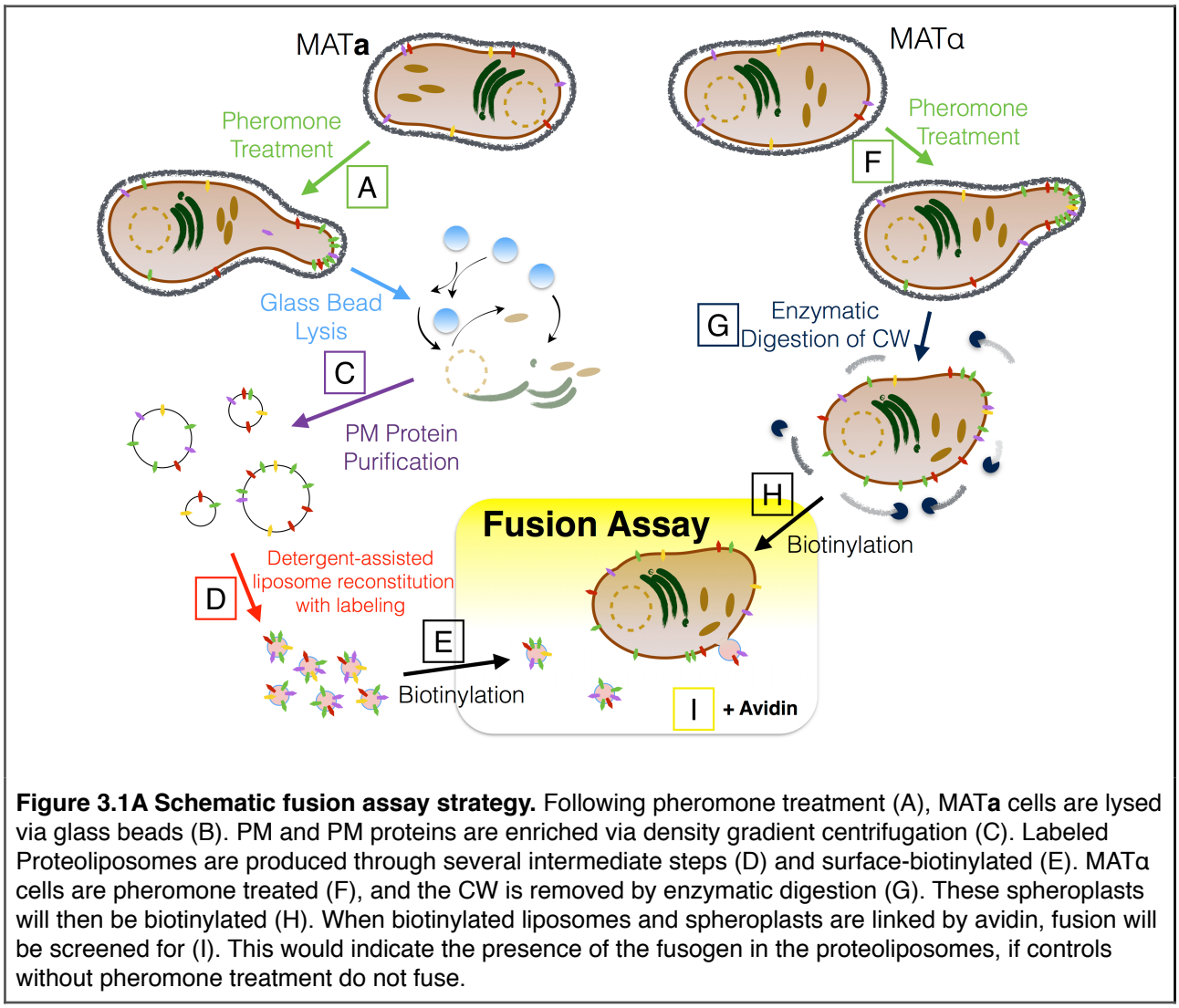

Figure 3.1A Schematic fusion assay strategy. Following pheromone treatment (A), MAT**a** cells are lysed via glass beads (B). PM and PM proteins are enriched via density gradient centrifugation (C). Labeled Proteoliposomes are produced through several intermediate steps (D) and surface-biotinylated (E). MATα cells are pheromone treated (F), and the CW is removed by enzymatic digestion (G). These spheroplasts will then be biotinylated (H). When biotinylated liposomes and spheroplasts are linked by avidin, fusion will be screened for (I). This would indicate the presence of the fusogen in the proteoliposomes, if controls without pheromone treatment do not fuse.

The conceived strategy for this project is depicted schematically on **Figure 3.1A**. The fusion assay will consist on the use of liposomes incorporating reconstituted PM proteins. These proteoliposomes will then be added to spheroplasts (cells with have had their CW removed by enzymatic digestion) derived from pheromone-treated cells of the opposite mating type. The ability

to control the properties of the proteoliposomes, including the protein density and liposome concentration, will enhance the probability that the reconstituted fusion machinery can interact with the machinery on spheroplasts and lead to fusion. To exclude the possibility of artifacts, both proteoliposomes and spheroplasts will be generated from pheromone-treated cells, thus ensuring that fusion is consistent with the pheromone dependency requirement of cells from both mating types. To evaluate fusion, proteoliposomes will be labeled with fluorescent lipid conjugates and contain encapsulated dye at a self quenching concentrations. Fusion will be monitored by microscopy as indicated by dilution of the dye within the cytoplasm of the spheroplast which will dramatically increase fluorescence. The outline of the part of assay development covered by this thesis is depicted in **Figure 3.1B**. The attachment assay resembles the final fusion assay on the side of the spheroplast preparation, although MAT**a** is used for practical reasons (for details refer to **3.1.3.**). Letters (A)-(F) refer to milestones in the development of the assay for this thesis.

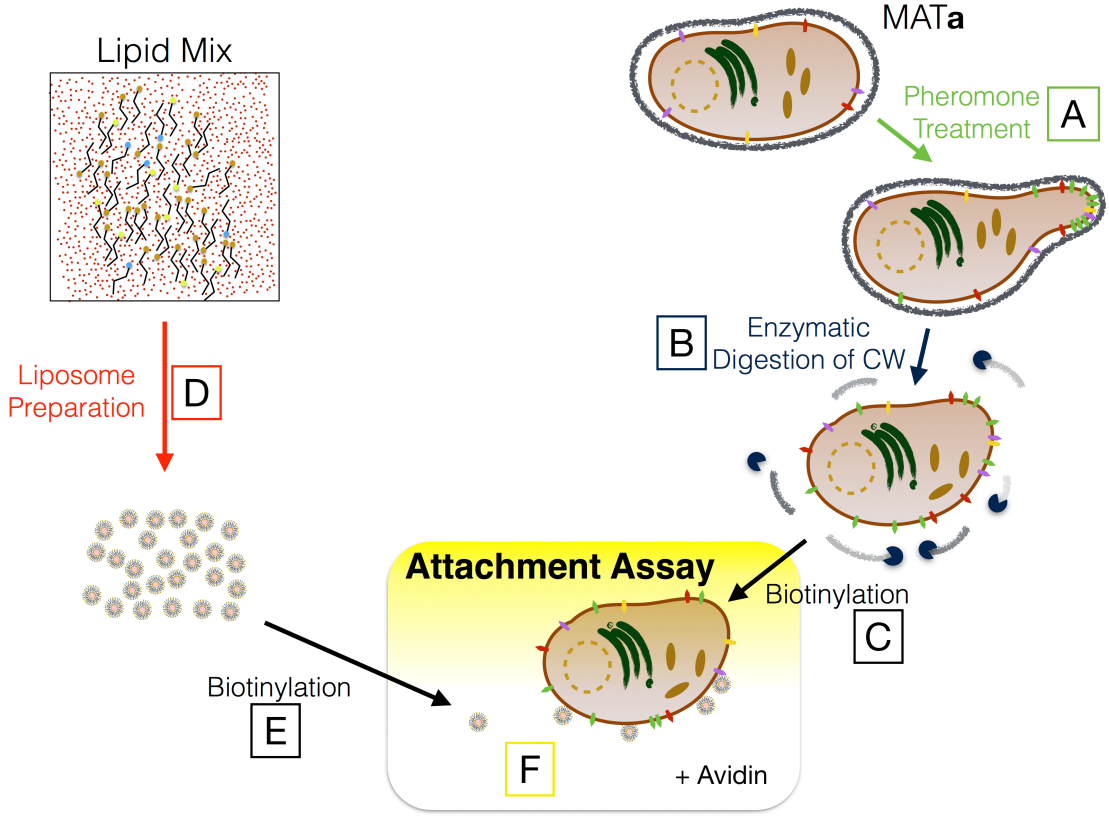

Figure 3.1B Schematic attachment assay development as covered by this thesis. MATα cells are pheromone treated (A), and the CW is removed by enzymatic digestion (B). These spheroplasts will be then surface-biotinylated (C). Liposomes will be produced from micellar solution of lipids (Lipid Mix) (D) and surface-biotinylated as well (E). When biotinylated liposomes and spheroplasts are linked by avidin, attachment conditions for fusion can be investigated (F).

It has long been known that spheroplasts are not able to fuse when they are pre-treated with pheromone [35]. The precise reason for why spheroplasts do not fuse are unknown. We hypothesize here that this is probably the consequence of PMs not being able to come into close contact. During mating, agglutinins in the CW ensure contact at the shmoos, a critical step for all downstream steps that follow at the PM. In the absence of agglutinin-like factors in spheroplasts, our approach will be to bring proteoliposomes and spheroplasts into close proximity using biotin-avidin linkage. For this there are different aspects which have to be optimized for a robust fusion assay: first, liposomes should only attach to spheroplasts when both are labeled by biotin and those biotins are linked by avidin. Tetrameric avidin has the ability to bind four biotins and

constitutes one of the strongest non-covalent bonds known [36]. Second, the kinetics of these reactions and the order in which they should take place have to be taken into account in the design of the fusion assay. Lateral diffusion of PM proteins might be another factor that may come into play as the localization of key proteins disperse over the entire cell surface after CW removal.

In this chapter, we will develop different aspects of the assay depicted in **Figure 3.1B**. This will include testing negative and positive controls for the proteoliposome-spheroplast fusion assay including the controlled attachment of liposomes to spheroplasts.

3.1. Characterization of pheromone response and spheroplasting

3.1.1. Pheromone response

For initiation of the mating process, haploid yeast cells are stimulated by a pheromone that is secreted by the opposite mating type: MAT**a** cells produce **a-**factor, which stimulates MATα cells. MATα cellsin turn produce α-factor triggering a response from MAT**a** cells, thus ensuring that only cells of opposite mating type mate and form diploid **a/**α cells. α-factor is a commercially available peptide of 13 amino acids, but unfortunately **a-**factor is not as easy to obtain. When comparing α-factor in **Figure 3.2A** with **a-**factor in **Figure 3.2B**, it becomes evident why that is the case: while α-factor is a mere polypeptide without any post translational modifications (and therefore readily synthesized), the C-terminal cysteine of the **a-**factor is both prenylated and methylated before it is secreted. Therefore, that **a-**factor was synthesized in-house by the peptide synthesis facility of the Max Planck Institute of Biochemistry using a modified protocol from O'reilly *et al*. [37]. This enabled us to reinvestigate previously published findings that are crucial for the establishment of the fusion assay.

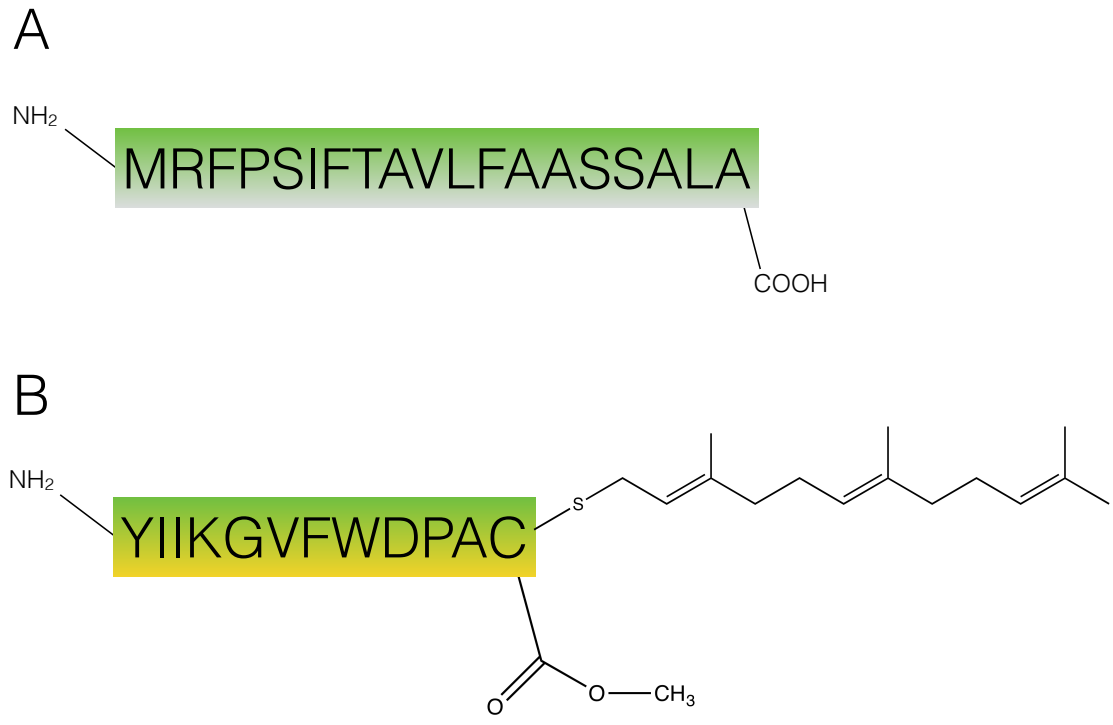

Figure 3.2 Yeast pheromones A) Mature α-factor, secreted by MATα cells is a simple peptide of 13 amino acids. **B)** Mature **a**-factor, secreted by MAT**a** cells is prenylated and methylated at the C-terminus.

3.1.1.1. Selection of MATa strain

To characterize the response of the chosen yeast strain to pheromone, cells were grown to a density of ~ 3 x 10^7 mL^{-1} and then transferred into fresh synthetic complete (SC) media with differing concentrations of either **a-**factor or α-factor. Morphological changes were evaluated at various time points. In response to pheromone treatment and in parallel to shmoo formation, budding was effectively blocked and thus halted asexual proliferation (data not shown).

The MAT**a** strain we use for our experiments is BJ5457 Δ*bar1* PRM1-GFP. This strain was selected and modified according to the following requirements: (1) the original BJ5457 strain is depleted of vacuolar proteases to safeguard against proteolytic degradation once cells are lysed [40]. (2) The deletion in the *BAR1* locus makes the strain significantly more sensitive to α-factor because it encodes a secreted protease that degrades α-factor. When *BAR1* is knocked out, the amount of pheromone required to induce shmoo formation is dramatically reduced (**Figure 3.3**) — rendering it possible to use the strain for large scale purification of PM proteins obtained from α-factor-treated cells. This is necessary since we require several liters of cell culture from the MAT**a** mating type and although α-factor is commercially available, it is not economically feasible to pheromone-treat such large quantities of cells in the presence of Bar1 activity. (3) The C-terminal GFP-tag of Prm1 enables us to quantify expression of Prm1, a protein that promotes cell fusion and is enriched at the shmoo (see **1.2.3.** for details). Expression of Prm1 is strictly pheromone-dependent, thus it can also be used as a marker for localization of components of the fusion machinery.

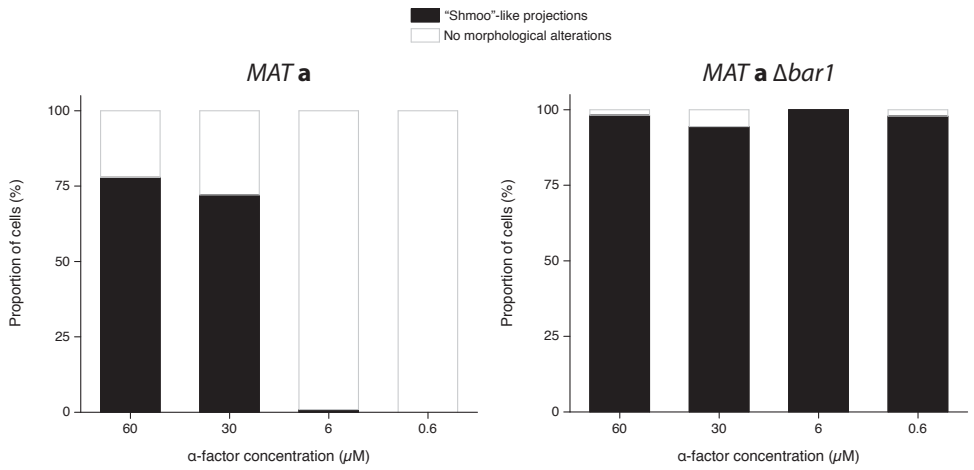

Figure 3.3 Effect of *BAR1* knock-out on α-factor sensitivity. Total cells and cells with shmoo projections were counted using a lightfield microscope after pheromone treatment. Cells deficient of Bar1 have a 50-fold increased sensitivity to α-factor. Additionally, responsiveness is also increased.

Time dependency of α-factor

In the fusion assay MAT**a** cells will be lysed by glass beads to purify and reconstitute PM proteins. This should be done when the pheromone response has been completed, ensuring that substantial amounts of fusion-related PM proteins are obtained. To determine this optimal time point for fusion experiments, pheromone response was investigated over time. Three distinct phases of pheromone response were distinguishable in MAT**a** cells:

- After incubation in SC media with α-factor for 3 h, prominent shmoo tips were observed on most of the cells (see **Figure 3.4B**). Noteworthy is also the partial polarization of Prm1 to the shmoo tip.
- After 6.5 h of incubation in SC media with α-factor, the overall level of fluorescence seemed to be even higher than after 3 h, translating into a higher level of Prm1 expression (see **Figure 3.4C**). However, secondary shmoos had begun to emerge by then.
- **Figure 3.4D** shows 20 h into the incubation with α-factor in SC media and revealed a considerable reduction in Prm1 expression. Morphology was severely affected with tertiary and even quaternary shmoo site formations.

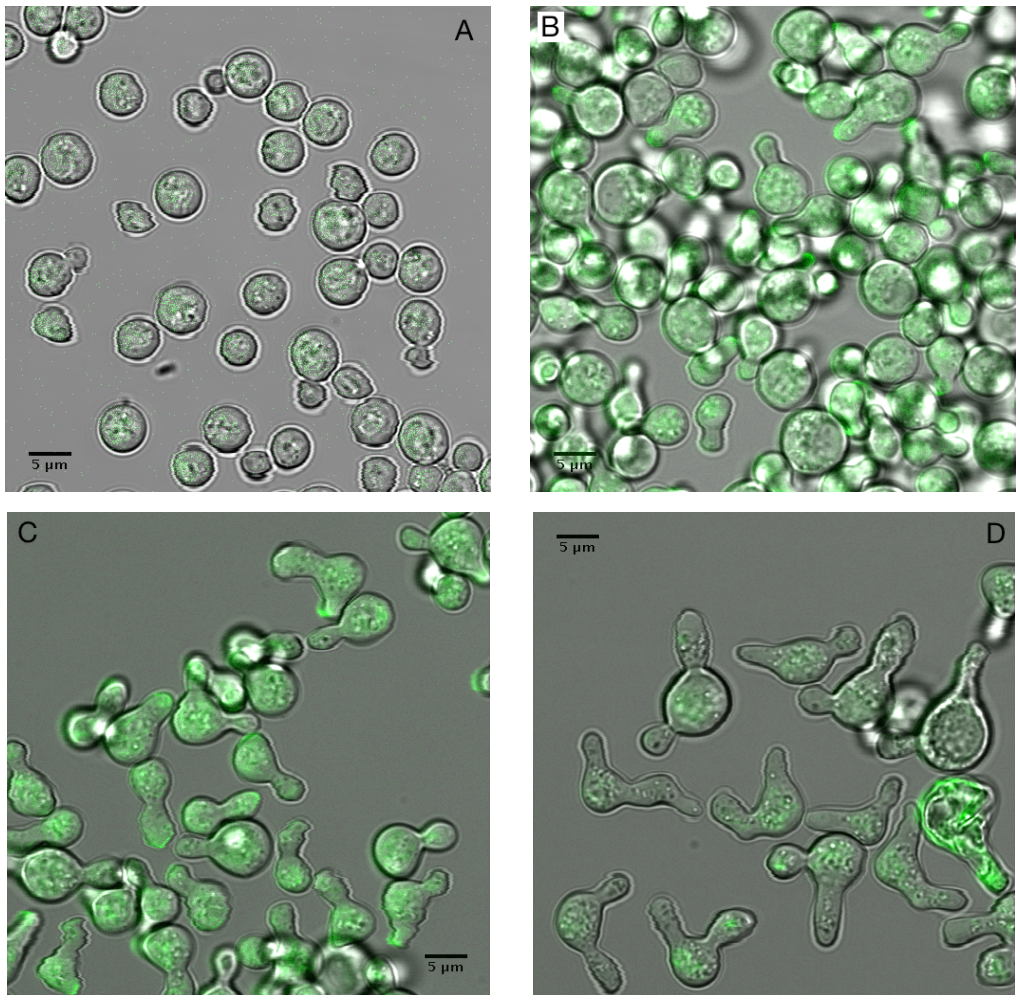

Figure 3.4 MATa ***PRM1*-GFP cells incubated with 0.5 *µ*g/mL α-factor.** Transmitted light and GFP emission overlay. Excitation at 488 nm. **A)** Control without α-factor after 6.5 h. Note the low auto-fluorescence and the noise. **B)** Incubated with α-factor for 3 h. Apparent shmoo formation with some polarization of Prm1 at the shmoo tip. **C)** Incubated with α-factor for 6.5 h. Higher overall Prm1 expression, formation of second shmoo with varying degrees of polarization. **D)** Incubated for 20 h. Multiple shmoo sites deform normal morphology.

These results indicate that the for our purposes optimal response to α-factor treatment is achieved after 3 h. Longer periods of pheromone treatment appear counterproductive as the cells lose polarization of Prm1 and undergo further morphological changes.

Concentration dependency of α-factor

Similar to the correlation of pheromone response to incubation time, the concentration dependency of α-factor was also evaluated. As **Figure 3.5** shows, there was no detectable difference in the pheromone response between concentration variations of 0.5 *µ*g/mL to 10 *µ*g/mL.

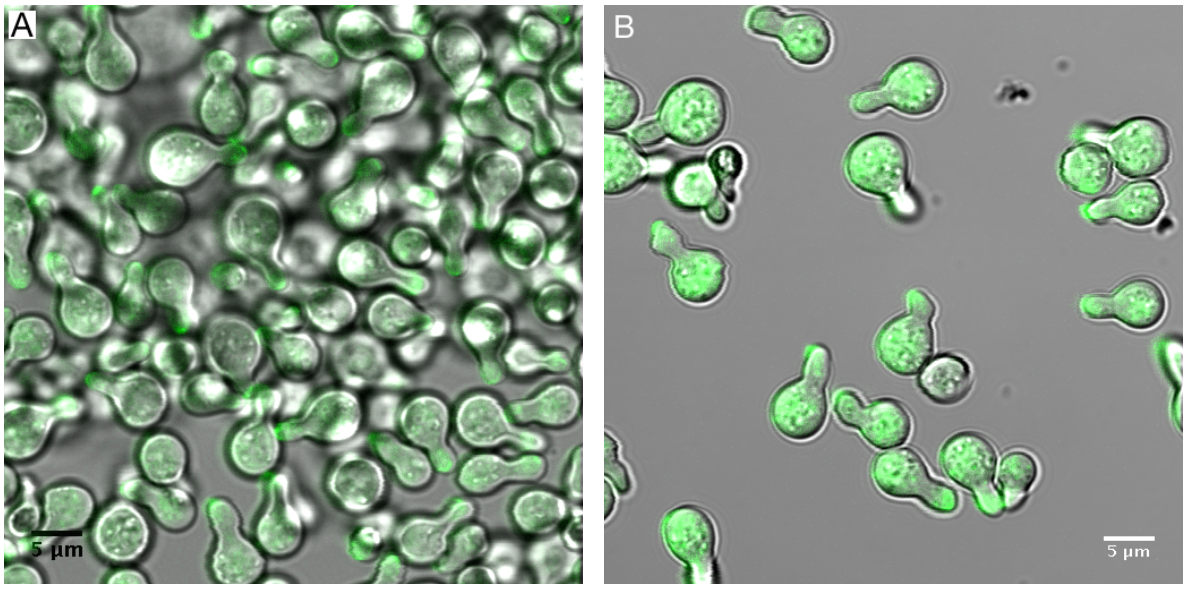

Figure 3.5 MATa ***PRM1*-GFP cells incubated with varying concentrations of α-factor for 3 h.** Transmitted light and GFP emission overlay. Excitation at 488 nm. **A)** Incubated with 0.5 *µ*g/mL α-factor. **B)** Incubated with 10 *µ*g/mL α-factor.

3.1.1.2. MATα

The MATα strain that is used in our experiments is BJ5459 [41]. Stimulation of MATα with **a**-factor has a few considerable differences to the situation with MAT**a**. First of all, there is no equivalent protease to Bar1, hence there is no need for a knock-out. But, as described in **3.1.1**, **a**-factor is not commercially available and had to be synthesized in-house, making it a valuable tool. Still, this does not only influence our work, but also affects other groups researching yeast pheromone response. This has led to limited published information and so we had to investigate pheromone response of MATα *de novo.*

Concentration dependency of a-factor

Effective stimulation requires understanding of the sensitivity to pheromone of the utilized yeast strain. MATα was stimulated by **a**-factor, synthesized in the core facility as described in **3.1.1.**.

We observed that the degree of response to pheromone in MATα seems more dependent on pheromone concentration as in the opposite mating type. As depicted in **Figure 3.6**, a concentration of 0.5 *µ*g/mL **a**-factor did not elicit obvious shmoo formation after 3 h of incubation in SC media (**Figure 3.6A**). 2.75 *µ*g/mL **a**-factor induced small morphological changes, presumably establishing shmoo sites, and 5 *µ*g/mL generated prominent shmoos after 3 h of induction (see **Figures 3.6B** and **C**), strongly resembling the MATa cells' response to pheromone, contrary to a

previous report [38]. A concentration of 25 μg/mL **a**-factor caused an abnormal morphology (**Figure 3.6D**), suggesting there is an optimal concentration between 2.75 μg/mL and 5 μg/mL.

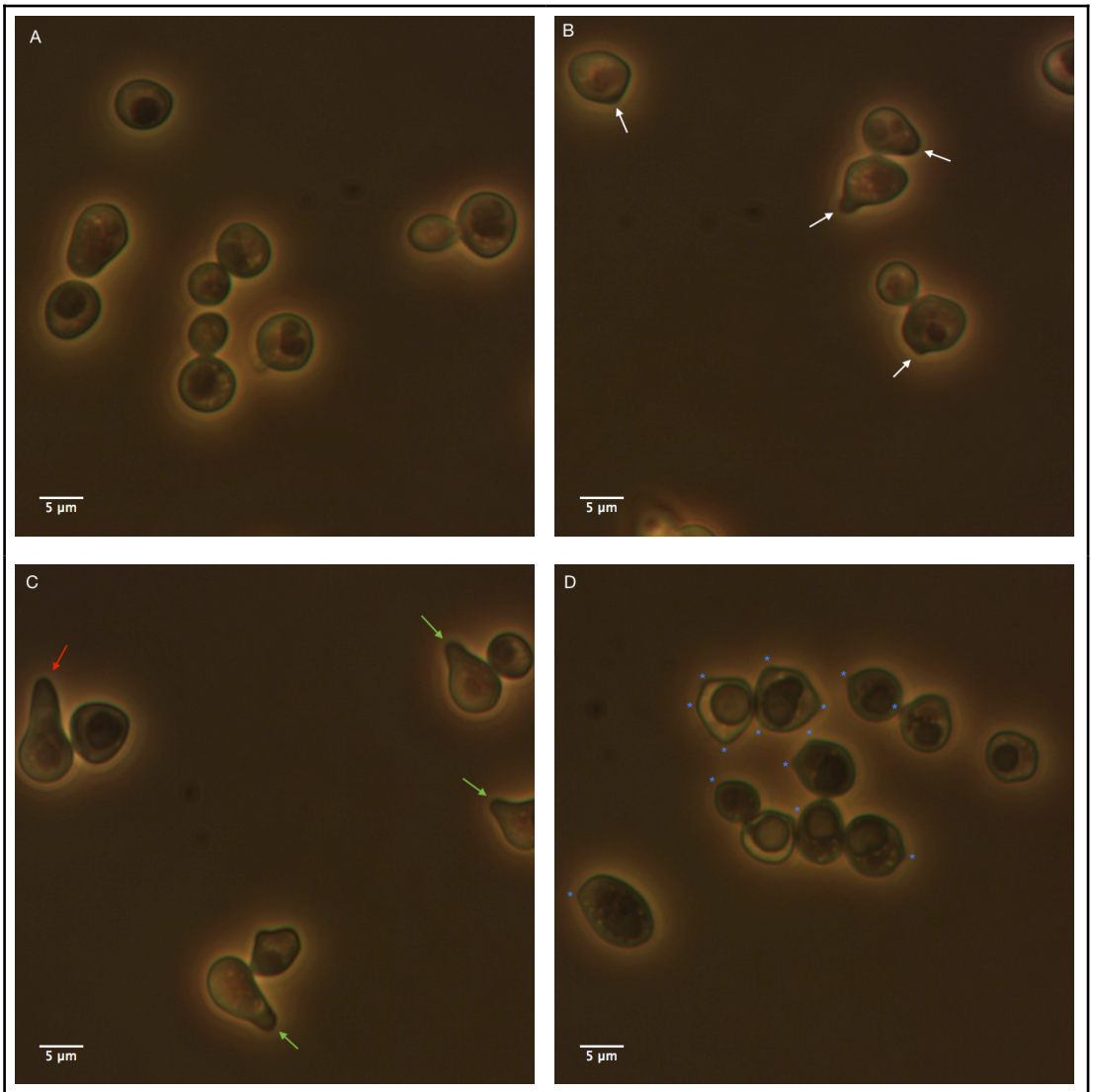

Figure 3.6 MATα cells treated with varying concentrations of a**-factor for 3 h.**
A) Treated with 0.5 μg/mL **a**-factor. **B)** Treated with 2.75 μg/mL **a**-factor, white arrows marking shmoo sites. **C)** Treated with 5 μg/mL **a**-factor, green arrows marking shmoo sites. Red arrow marks extraordinarily large shmoo. **D)** Treated with 25 μg/mL **a**-factor. Blue asterisks mark abnormal shmoo formation.

3.1.2. Generation of spheroplasts

It was necessary to characterize appropriate spheroplasting conditions since they form an essential part of our proposed fusion assay. Spheroplasts were generated using the BJ5457 MAT**a** Δ*bar1* PRM1-GFP strain via addition of Zymolyase 100T under osmotic support, in our case a buffer with 1 M Sorbitol, 20 mM PIPES, pH 7.5 (henceforth Spheroplasting Buffer). 30 min of treatment at 35 °C with occasional, very gentle mixing with a pipette were enough to produce spherical cells that were susceptible to osmotic lysis

Note that in the final assay we will utilize spheroplasts derived from MATα cells. However, for characterization purposes we used a MAT**a** strain providing general insights that can be applied to MATα cells as well.

3.1.2.1. Osmotic lysis test

One way to test for sufficient spheroplasting is by applying an osmotic shock. Since spheroplasts lost their CW due to enzymatic degradation, they are unprotected against SDS. SDS partially solubilizes the lipids of the PM, resulting in bursting of the cells. After cells underwent the spheroplasting procedure, 5 μL of the sample was applied to an object slide and mixed with 1 μL of 20% SDS Buffer. The spheroplasts lysed and debris that was rarely detectable had different phase shift than viable yeast cells (compare **Figure 3.7A** and **B**).

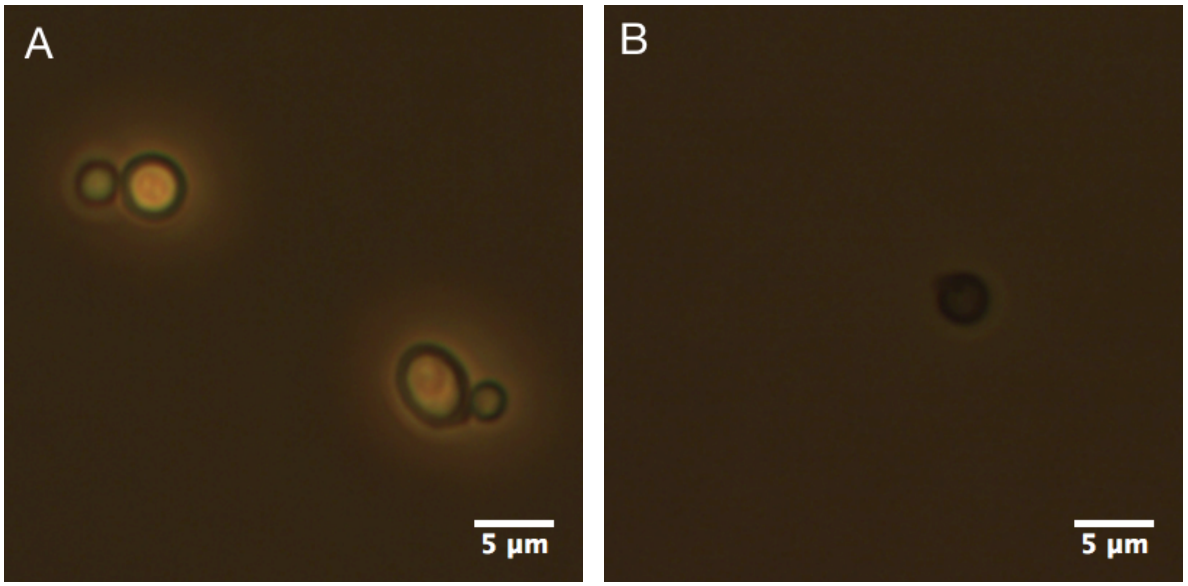

Figure 3.7 Osmotic lysis test. A) MAT**a** cells after spheroplasting. **B)** MAT**a** cells after spheroplasting and subsequent addition of SDS to a final concentration of 4 %.

With these experiments we were able to assess the crucial success of the spheroplasting procedure in the following experiments.

3.1.3. Comparison between pheromone-treated spheroplasts versus spheroplasting of pheromone-treated cells

To assess pheromone response and the behavior of spheroplasts, we once again used BJ5457 MAT**a** Δ*bar1* PRM1-GFP instead of MATα. The decision to not use a MATα strain in the first place is based on a practical consideration: at the time of the experimental work of the thesis we only had a MAT**a** strain with a GFP-tag at the Prm1. The possibility to track Prm1 expression and targeting was essential to be able to evaluate the outcome of our experiments. Furthermore, during the course of experiments we needed to use reasonable large amounts of pheromone. As already explained above, α-factor is easier available. Nevertheless, since Prm1 has the same function in MATα, the results should be applicable to the other mating type as well.

3.1.3.1. Impact of spheroplasting on the Prm1 distribution in pheromone-treated MATa cells

We noticed that spheroplasts derived from pheromone-treated MAT**a** cells lost a substantial part of Prm1-GFP polarization during the spheroplasting procedure (data not shown). In order to determine the causes we examined cells during the different steps of the initial spheroplasting procedure (containing several washing steps in ultra pure water) and checked for fluorescence and polarization of Prm1-GFP.

Figures 3.8A-C show the relevant controls for this experiment: cells before and after spheroplasting without prior pheromone treatment (**Figures 3.8A** and **C**, respectively), and normally pheromone-treated cells in SC media (**Figure 3.8B**) that fluoresce strongly and in a polarized manner. The level of fluorescence changes remarkably with the amount of stress applied to the cells: after the first centrifugation at 2500 rcf for 2 min the cells appear less fluorescent, although polarization is still evident (**Figure 3.8D**). Subsequent steps (**Figures 3.8E-G**) do not aggravate the loss of fluorescence, however, polarization at the shmoo is considerably reduced. The shmoos are well-preserved even after CW removal. Other experiments confirmed this, though the shmoos appeared a little more spherical, too. These findings suggest intracellular filaments are at work, supporting the shmoo structure as a scaffold. However, they seem particularly depleted from Prm1-GFP, suggesting possible internalization and degradation.

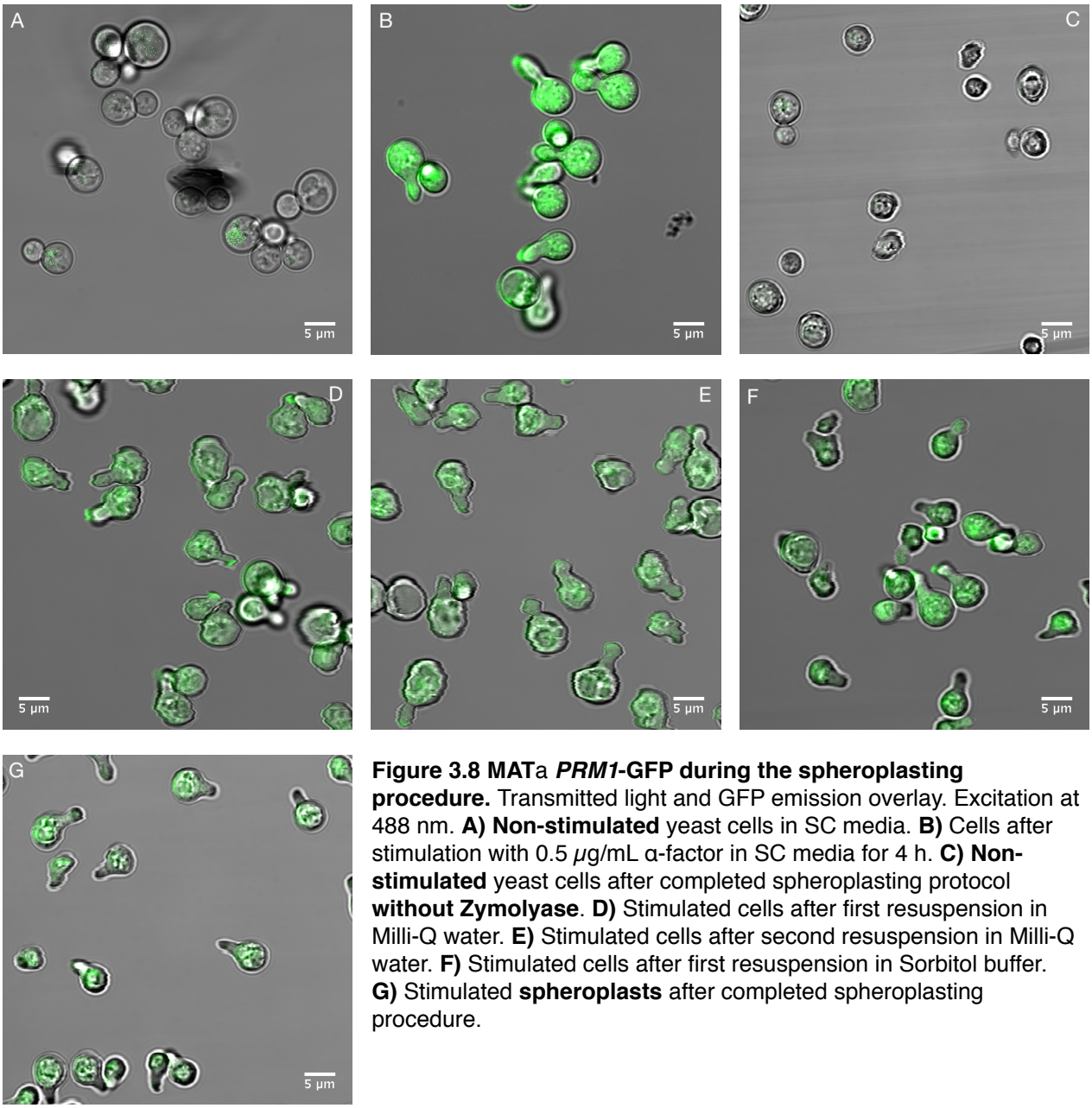

Figure 3.8 MATa ***PRM1*-GFP during the spheroplasting procedure.** Transmitted light and GFP emission overlay. Excitation at 488 nm. **A) Non-stimulated** yeast cells in SC media. **B)** Cells after stimulation with 0.5 µg/mL α-factor in SC media for 4 h. **C) Non-stimulated** yeast cells after completed spheroplasting protocol **without Zymolyase**. **D)** Stimulated cells after first resuspension in Milli-Q water. **E)** Stimulated cells after second resuspension in Milli-Q water. **F)** Stimulated cells after first resuspension in Sorbitol buffer. **G)** Stimulated **spheroplasts** after completed spheroplasting procedure.

Still, the design of the assay aims to obtain both a high overall expression of proteins of the fusion machinery and a targeted localization of those to the shmoo. As a consequence of these results, we sought to reduce the effects of spheroplasting on pheromone-treated cells. We hypothesized that depolarization is as a result from the stress that centrifugation exerts on the cells during the washing steps. Therefore we investigated the cells' response to pheromone in different media and whether choice of media can alleviate depolarization of Prm1-GFP.

If shear stress at the shmoo was responsible for internalization of Prm1, we guessed that more viscous media might improve the spheroplasts ability to maintain Prm1 polarization. Compared to treatment with pheromone in SC media only (**Figure 3.9A**), the response in buffer that consists of 50 % v/v regular SC media and 50 % Spheroplasting Buffer (50/50 Buffer) was similar (**Figure 3.9C**). Almost no Prm1-GFP and shmoo formation was detected in cells in Spheroplasting Buffer (**Figure 3.9B**). As expected, this did not change after centrifugation (**Figure 3.9E**). Analogous to the results depicted in **Figure 3.8** the shearing forces affecting the

cells during centrifugation gave rise to depolarization of Prm1 (**Figure 3.9D**) which could largely not be prevented by the additional osmotic support from the 50/50 Buffer (see **Figure 3.9F**).

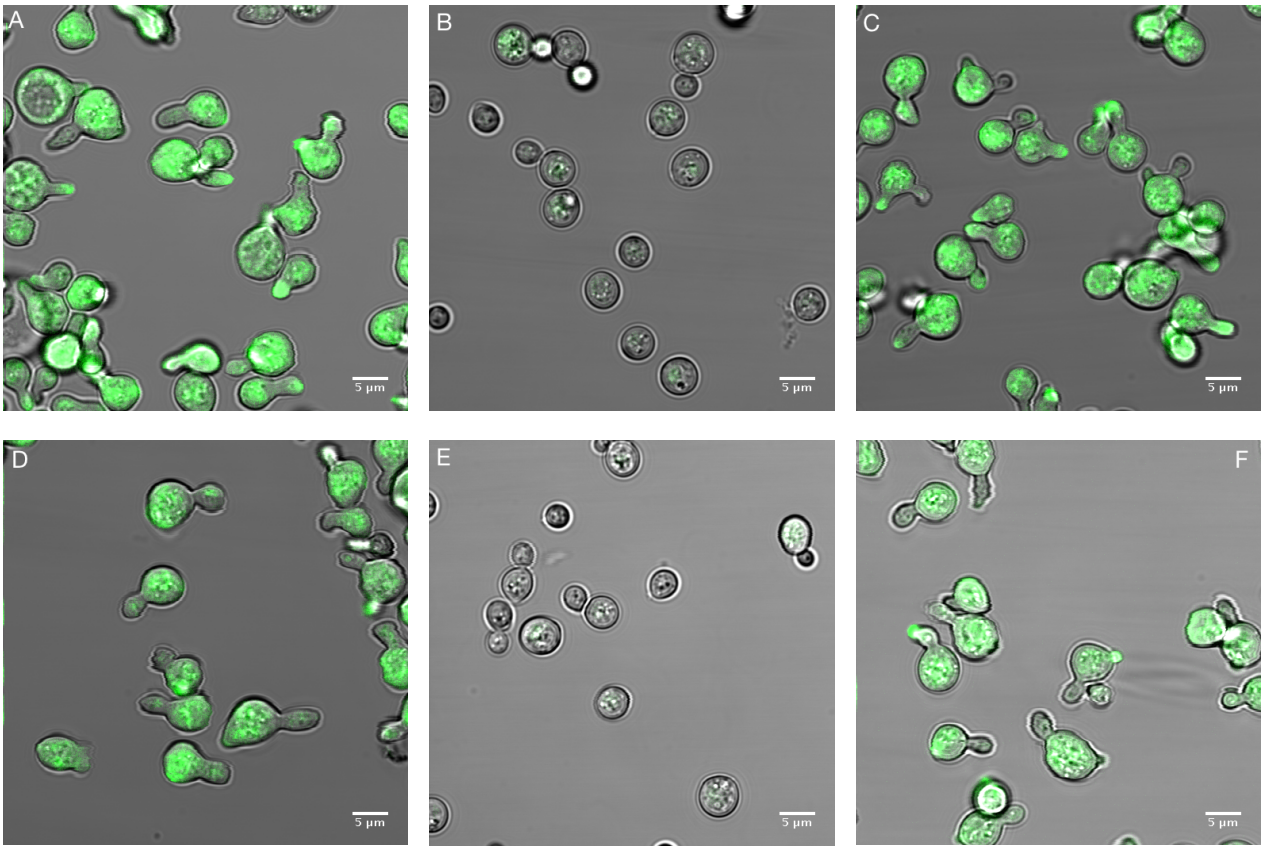

Figure 3.9 MATa ***PRM1*-GFPs response to stimulus in different media and effect of centrifugation on possible internalization.** Transmitted light and GFP emission overlay. Excitation at 488 nm. **A)** Cells after stimulation with 0.5 µg/mL α-factor for 4 h in **SC media**. **B)** Cells after stimulation with 0.5 µg/mL α-factor for 4 h in **Spheroplasting Buffer**. **C)** Cells after stimulation with 0.5 µg/mL α-factor for 4 h in **50/50 Buffer**. **D)** Stimulated cells after centrifugation at 2500 rcf, both in **SC media**. **E)** Stimulated cells after centrifugation at 2500 rcf, both in **Spheroplasting Buffer**. **F)** Stimulated cells after centrifugation at 2500 rcf, both in **50/50 Buffer**.

3.1.3.2. Pheromone response in spheroplasts

The loss in polarization of Prm1-GFP in cells during the spheroplasting procedure is a potential problem for the investigation of fusion with our proposed fusion assay. Because of this, we decided to examine whether spheroplasts can themselves respond directly to pheromone treatment. The previous experiment (compare **Figure 3.9**) revealed that cells need metabolic nutrients in order to respond to pheromone. Additionally, spheroplasts might require osmotic support to prevent them from becoming protoplasts by peeling of residual CW [39]. This could cause lysing during subsequent washing steps that become necessary as the development of the fusion assay proceeds. Furthermore, it is not clear if our proposed fusion assay in the end might need residual CW as provided by spheroplasts.

Consequently, we speculated that 50/50 Buffer can be used for the pheromone-treatment of spheroplasts. Indeed, spheroplasts appeared as viable when transferred to 50/50 Buffer instead of SC media after spheroplasting (**Figure 3.10**). This result prompted us to investigate pheromone response in spheroplasts first prepared in Spheroplasting Buffer followed by pheromone-treatment with α-factor in 50/50 Buffer.

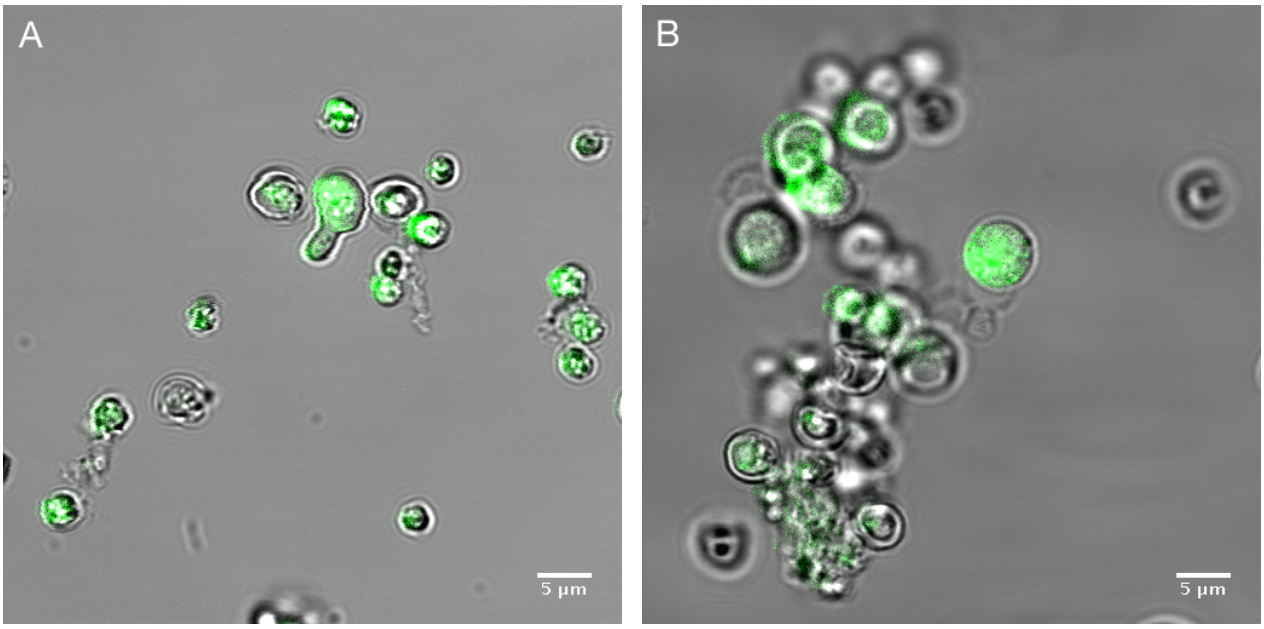

Figure 3.10 Pheromone response after spheroplasting. Transmitted light and GFP emission overlay. Excitation at 488 nm. **A)** MAT**a** *prm1*-GFP spheroplasted in Spheroplasting Buffer and stimulated in SC media. **B)** MAT**a** *prm1*-GFP spheroplasted in 50/50 Buffer and stimulated in 50/50 Buffer.

A time lapse experiment revealed the kinetic properties of the response of spheroplasts to pheromone, as shown in **Figure 3.11**. The rather poor contrast in the image is due to minimization of excitation laser power to prevent bleaching. This result suggests a response lag time comparable to non-spheroplasted cells. Surprisingly, **Figure 3.11B** also demonstrates that spheroplasts show a polarization of Prm1.

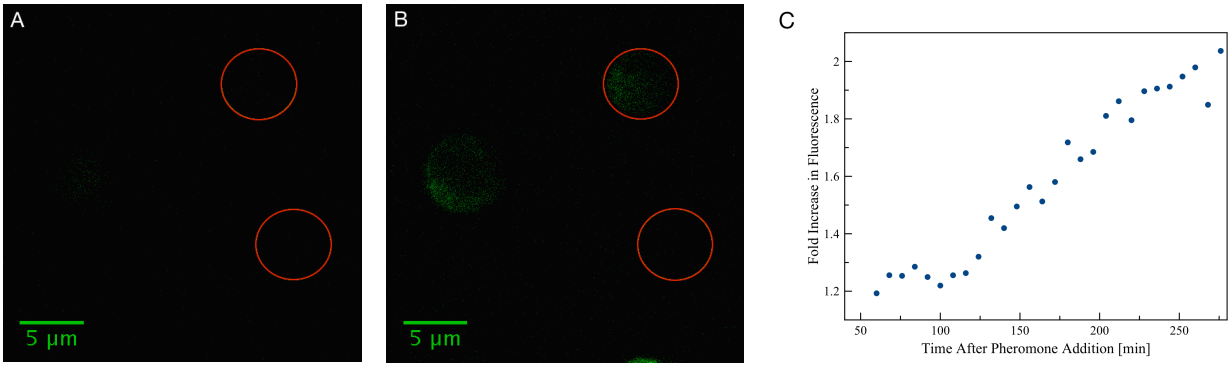

Figure 3.11 MATa ***PRM1*-GFP pheromone response in spheroplasts over time.** Pheromone treatment in 50/50 Buffer. Upper red circle represent the surveyed spheroplast, lower red circle served as a reference to which the values in ***C)*** were normalized. Excitation at 488 nm. **A)** Spheroplasts at the beginning of measurement, 60 min after α-factor addition of 0.5*µ*g/mL. **B)** Spheroplasts at the end of measurement, 276 min after α-factor addition of 0.5 *µ*g/mL. **C)** Graph showing increase in fluorescence of the surveyed spheroplast over time. Normalized to reference area.

Additional time lapse experiments of readily stimulated spheroplasts showed that polarized Prm1 fluctuates over the entire cell surface (**Figure 3.12**).

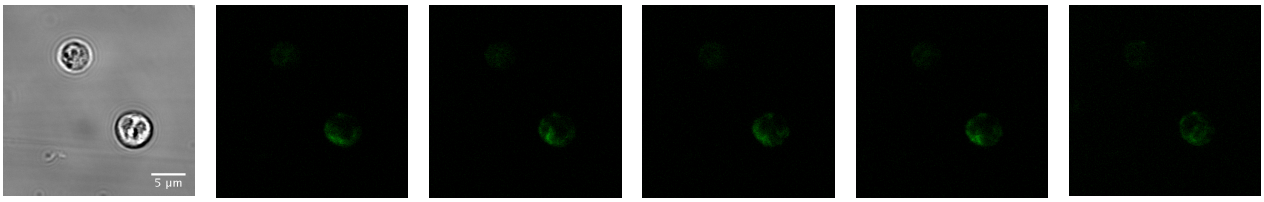

Figure 3.12 Fluctuation of Prm1-GFP over surface of spheroplast. BJ5457 MAT**a** Δ*bar1* PRM1-GFP, over a course of ~5 min. Leftmost image shows transmitted light. Excitation at 488 nm.

Due to these findings we decided to change our plans accordingly and utilize pheromone-treated spheroplasts as opposed to spheroplast pheromone-treated cells.

3.2. Biotinylation of spheroplasts

We reversed the initially intended order of steps as presented in **Figure 3.1B** — both spheroplasting and subsequent biotinylation are now prior to pheromone treatment — because of the findings in **3.1.3.1.**. Proteins that are targeted to the PM as a response to pheromone treatment, such as Prm1 and other proteins of the fusion machinery, will not be biotinylated as a consequence. The reversed order has thus the secondary effect that this might circumvent potential problems from biotinylation of proteins required for fusion.

3.2.1. Assessment of biotinylation efficiency

Biotin-avidin (or biotin-streptavidin) linkage were used to prolong the contact time and consequently possible interaction between the liposomes and the spheroplasts. Therefore an important goal to be met was the reliable, effective and reproducible biotinylation of the spheroplasts.

3.2.1.1. Western blot

The western blot in **Figure 3.13** shows biotinylation of membrane proteins of both cells and spheroplasts, investigated via a streptavidin-horseradishperoxidase conjugate.

Cells were partially pheromone-treated (lysates in lanes 5-8). Following this, half of the samples were spheroplasted with Zymolyase 100T (lysates in lanes 2, 4, 6 and 8) and afterwards four samples were treated with proteinase K (lysates in lanes 3, 4, 7 and

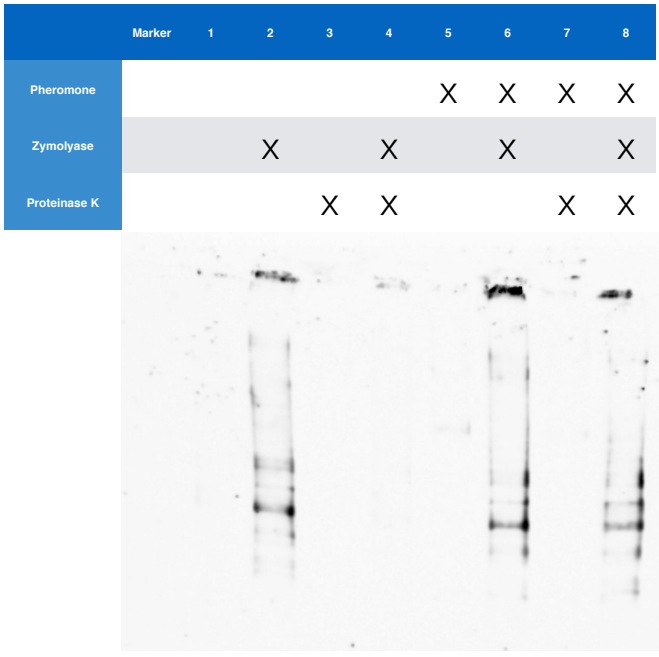

Figure 3.13 Westernblot to assess biotinylation efficiency. Marker did not transfer. Lanes 5-8 contained lysates from samples that had been pheromone-treated. Lysates in lanes 2, 4, 6 and 8 contained samples that had been spheroplasted and lanes 3, 4, 7 and 8 contained lysates from samples that had been treated with proteinase K.

8). Proteinase K is a broad-spectrum serin proteinase and should therefore effectively shear PM proteins. Thus one would expect no bands in the lanes were proteinase K was applied to the sample. The transfer of the protein weight marker failed and lane 8 shows biotinylated proteins regardless of proteinase K treatment before biotinylation. As a consequence of this poor result, we devised another method to test for biotinylation efficiency using a streptavidin-fluorophor conjugate.

3.2.1.2. Streptavidin Alexa Fluor 555 conjugate

Biotinylation was additionally evaluated with confocal microscopy via labelling with Alexa Fluor 555. **Figure 3.14** illustrates that only biotinylated spheroplast showed enrichment of the fluorescent dye in their CW.

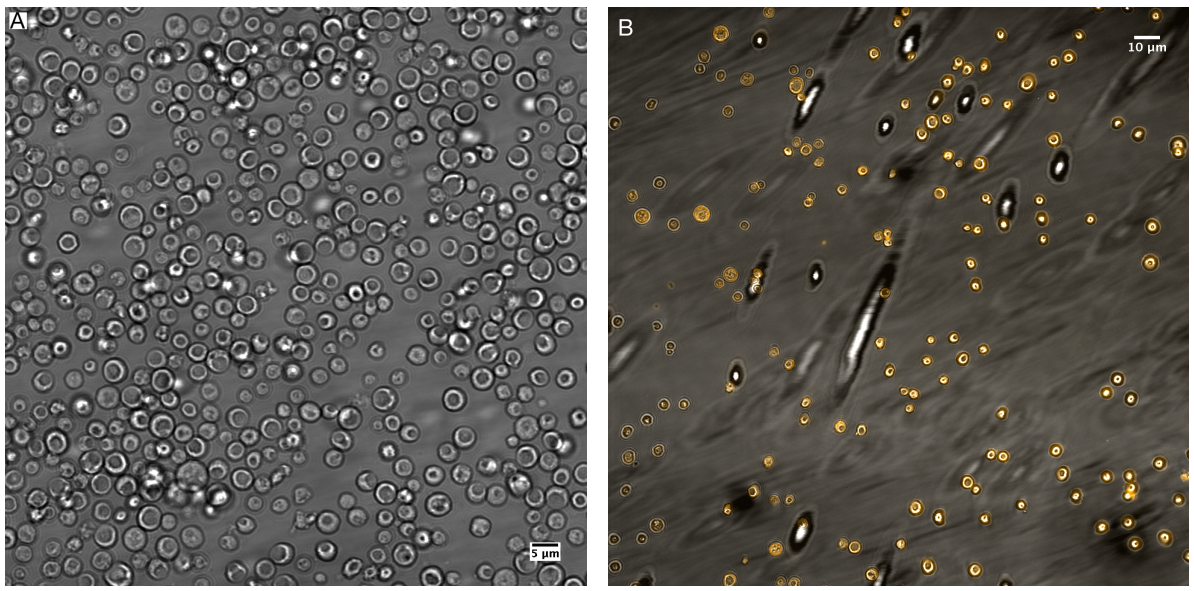

Figure 3.14 Spheroplasted MATa **cells with 25 µg/mL streptavidin Alexa Fluor 555.** Both are excited at 543 nm and show transmitted light and emitted fluorescence as an overlay. **A)** Non-biotinylated spheroplasts **B)** Biotinylated spheroplasts.

3.2.2. Biotinylation of pheromone-treated spheroplasts

Following this, it was necessary to demonstrate that our biotinylation procedure does not affect or limit the pheromone response of the spheroplasts. It is possible that PM proteins that have been biotinylated may adversely affect Prm1 targeting to the PM. Likewise it could be that pheromone-treatment may influence the distribution of the biotinylated proteins at the PM.

To test this we examined spheroplasts in four different conditions: (**Figure 3.15A**) Non-biotinylated, non-pheromone-treated vs. (**Figure 3.15B**) non-biotinylated, pheromone-treated vs. (**Figure 3.15C**) biotinylated, non-pheromone-treated vs. (**Figure 3.15D**) biotinylated, pheromone-treated. The results suggest that both reactions are independent from one another and thus neither pheromone-treatment affects the distributionn of biotinylated surface proteins nor does biotinylation prevent expression and targeting of Prm1 to the PM.

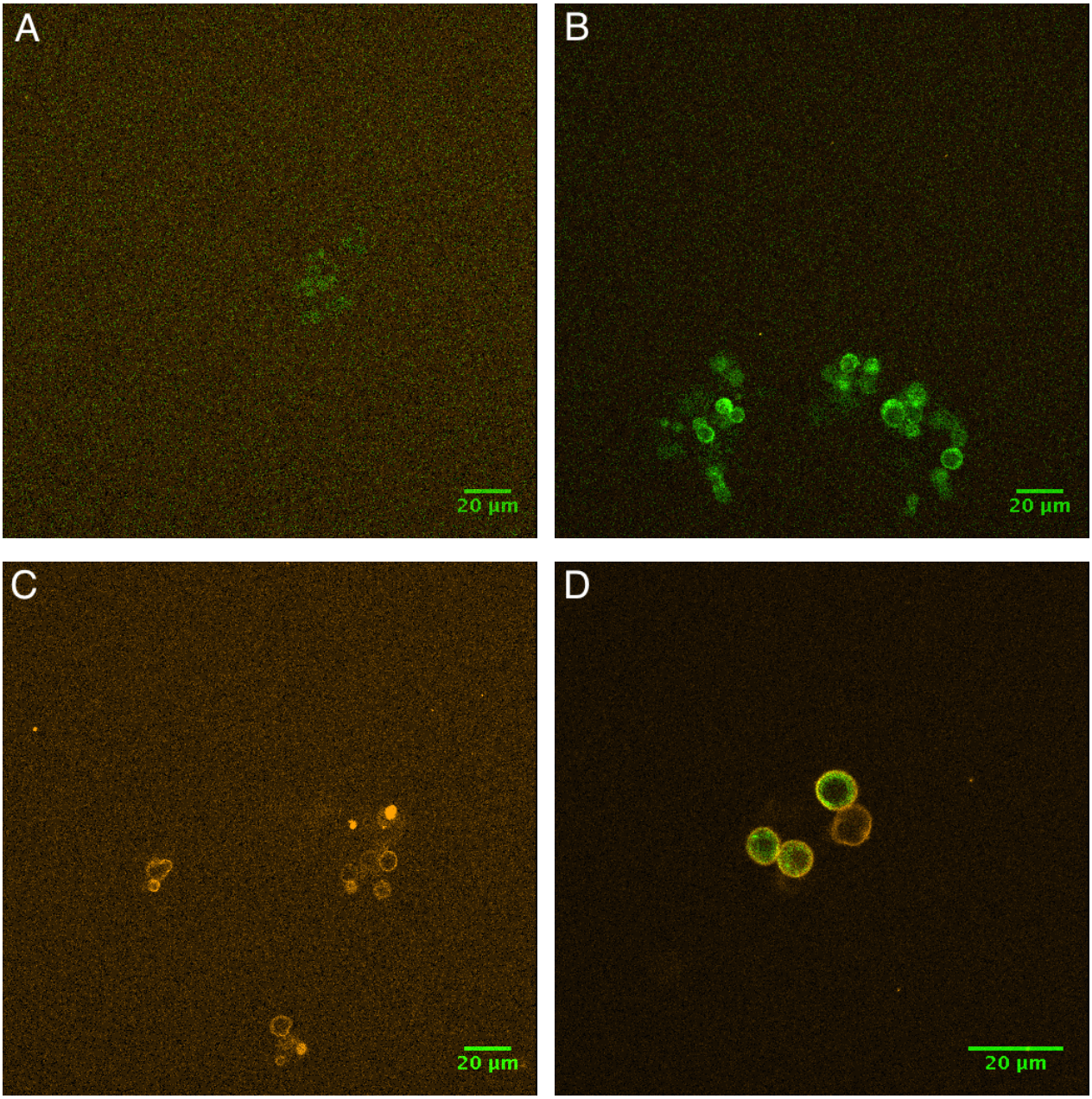

Figure 3.15 Investigating possible effects of biotinylation on pheromone response. Biotinylation was examined via streptavidin Alexa Fluor 555 conjugate. Excitation at 543 nm and 488 nm. Images show overlay of GFP and Alexa Fluor 55 emission. **A)** Non-biotinylated, non-pheromone-treated spheroplasts. **B)** Non-biotinylated, pheromone-treated spheroplasts. **C)** Biotinylated, non-pheromone-treated spheroplasts. **D)** Biotinylated, pheromone-treated spheroplasts.

3.3. Liposome Preparation Procedure

The liposomes that shall be used in the final fusion assay will contain reconstituted PM proteins, making them proteoliposomes. Preliminary work requires the characterization of attachment of protein-free liposomes to spheroplasts. Since there is no spontaneous interaction between plain liposomes and spheroplasts, we decided to utilize biotin-(strept)avidin linkage to enhance attachment between both membranes. In the following section we will show the steps taken to produce liposomes of 35-120 nm in diameter, labeled both by a fluorescent lipid conjugate and an encapsulated dye.

3.3.1. Lipid mix preparation

Lipid Mix was prepared by pipetting the respective lipids into a glass vial, drying under N_2, and redissolved it in Lipid Mix Buffer. With 0.4 M D-Sorbitol, 0.2 M NaCl, 0.02 M HEPES, 0.1 M Sulforhodamine B and 5 % or 2% CHAPS, the Lipid Mix then had the same osmolality as the Elution/Dialysis Buffer. Sulforhodamine B was present in self-quenching concentration so that fluorescence would dramatically increase upon release of the dye. This will be crucial for assessment of fusion.

3.3.2. Development of the liposome preparation protocol

The procedure of liposome preparation was modified and refined throughout the experimental work for this thesis. We changed Lipid Mix composition as well as concentration, utilized 3 different columns and applied rapid dilution as well as dialysis for generating liposomes. The ultimate goal was to obtain enough yield and high dye encapsulation efficiency for the fusion assay.

3.3.2.1. Lipid mix composition

We made several alterations to the Lipid Mix to adjust for experimental data, but the general composition consisted of the lipids 1-Palmitoyl-2-oleoylphosphatidylcholine (POPC) and 1,2-palmitoyl-oleoyl-*sn*-glycero-3-phosphoserine (POPS). We changed the percentage of ATTO655 from initially 1 % to 0.2 % (n/n), because the fluorescence signal was too high. The fourth lipid was 1,2-dipalmitoyl-*sn*-glycero-3-phosphoethanolamine-N-(cap biotinyl) (16:0 Biotinyl Cap PE), providing the liposomes with surface exposed biotin to which (strept-)avidin could bind. We started with a concentration of 0.1% 16:0 Biotinyl Cap PE and increased it to a final 2 % (see **Tables 2.5** and **2.6** for details).

3.3.2.2. Dialysis

Both to improve yield and encapsulation of Sulforhodamine B, we tried to utilize dialysis for our purposes. However, it was proven insufficient in removing enough CHAPS to get below the CMC, no matter how big the dialysis volume and duration. Experiments with dialysis only in Dialysis Buffer showed no encapsulation of dye whatsoever. In another approach, Sulforhodamine B was added to osmolality adjusted Dialysis Buffer. This yielded liposomes with encapsulated dye, but according to fluorometric measurements, not at self-quenching concentration.

3.3.2.3. Gel filtration liposome preparation and purification

The ÄKTApure size exclusion chromatography system from GE Health was used in the beginning for liposome preparation based on a previously published strategy [42].
Lipid Mix was introduced via an injection loop and a flow of Elution Buffer transports the sample to the column. The rationale is that due to the fact that both lipids and liposomes are way above

the size exclusion limit, they will pass the column considerably faster than Sulforhodamine B and CHAPS.
When the detergent is separated from the lipids, lipid bilayers form. If there is still sulforhodamine B present, it gets encapsulated. Exterior dye is separated is well. Fractions are collected and the ones containing liposomes, as detected by the UV detector and shown in the flow diagram, are used for characterizing and conducting downstream experiments.

First column

The column we initially used was a GE Healthcare Life Sciences HiTrap Desalting column. The details for the ÄKTApure method for this and the other preparations can be found in **Tables 2.7.**, **2.8.** and **2.9.**.

Indeed **Figure 3.16** shows a high peak in fluorescence and a relatively small preceding peak. We speculated that this would be liposomes followed by the excess Sulforhodamine B. The results suggested that a portion of liposomes might have encapsulated dye, due to the bad resolution between the two populations.

Investigating the particle size of the yielded liposomes, we examined them via Dynamic Light Scattering (DLS). As a result, we found that the average diameter of the liposomes was ~ 35 nm, but also widely distributed.

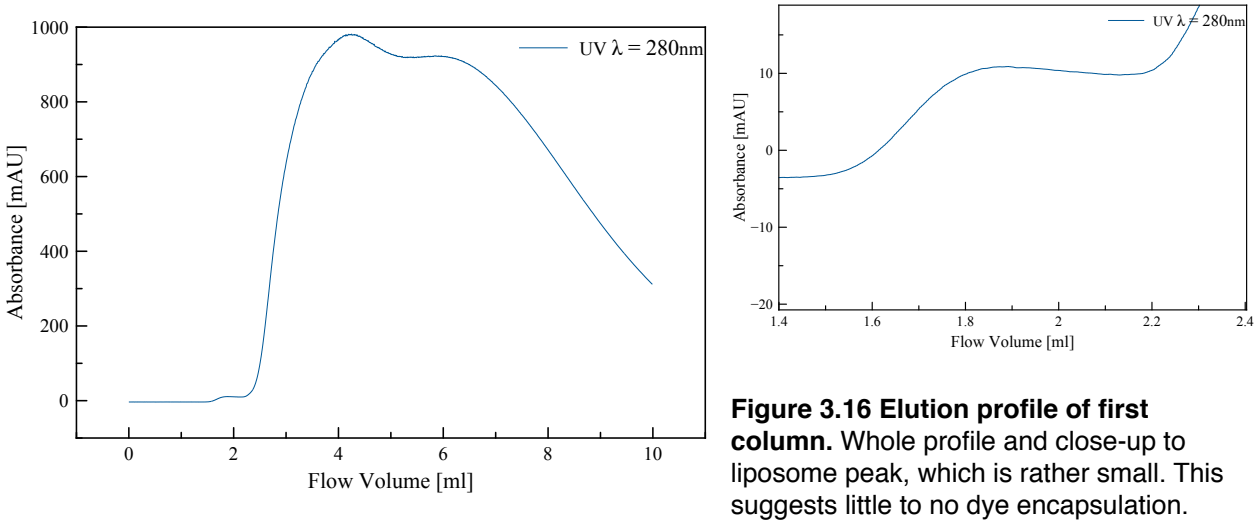

Figure 3.16 Elution profile of first column. Whole profile and close-up to liposome peak, which is rather small. This suggests little to no dye encapsulation.

We assessed the encapsulation by fluorometric analysis. Liposomes were solubilized after application of SDS, releasing encapsulated dye. If the dye was encapsulated at self-quenching concentration, the fluorescence should dramatically increase due to dilution. However, it seems that the dye was separated before the detergent concentration decreased under the CMC. Thus the liposomes did not encapsulate considerable amounts of dye (data not shown).

Second column

In search of a column that would yield substantial quantity of liposomes containing encapsulated dye, we tried the larger Superdex™ Peptide 3.2/300 column. Following the observation that the liposomes do not encapsulate dye with the previous method, the column was thenceforth used solely for purification purposes, that is removing detergent and excess dye from

the liposomes. The liposomes were generated through Rapid Dilution, which in turn strongly limited our yield. Rapid Dilution decreases the CHAPS concentration of the lipid mix to 0.25% (w/v) or lower and thus under the CMC. Naturally this also drastically dilutes the lipid concentration. Since the volume that can be applied to a gel filtration column is limited, this leads to a low yield of liposomes in the end.

Figure 3.17 shows the flow diagram as recorded by the ÄKTApure. The separation of liposomes and dye is evident. In the meantime we had purchased an additional UV detector so we could discern fluorescence signal of the dye (λ = 565 nm) from the signal obtained by lipids. Both UV detectors record a signal at 1-1,15 mL of elution volume (see close-up in **Figure 3.17**), suggesting encapsulated dye. The purification of liposomes that have been prepared the same way except without Sulforhodamine B is presented in **Figure 3.18**. Note the absence of signal detected by UV2 and the lower overall fluorescence.

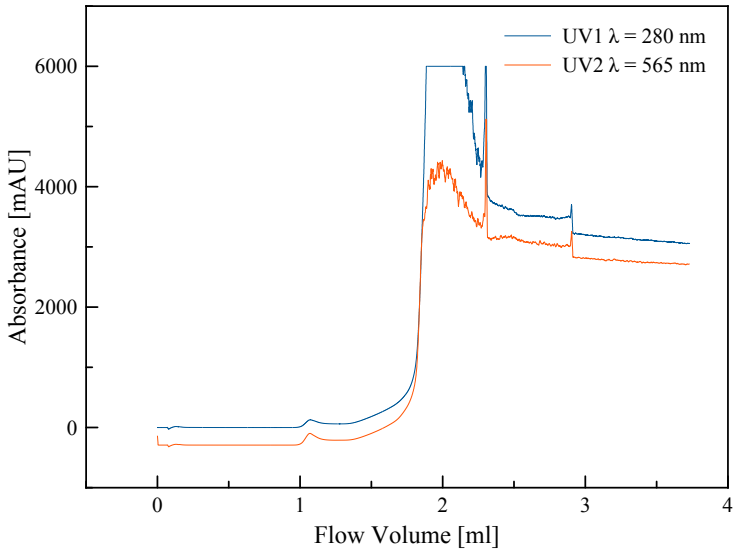

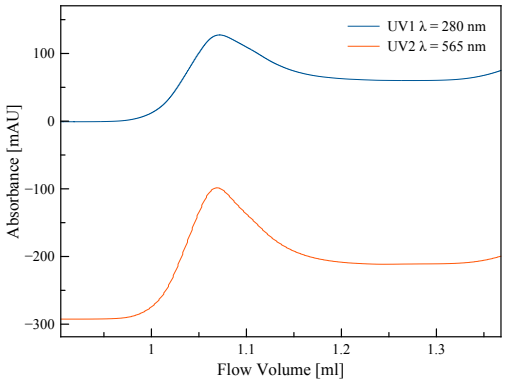

Figure 3.17 Elution profile second column. Liposome preparation in presence of dye. Whole profile and close-up to liposome peak. Large amplitude and overlap with UV2 suggest dye encapsulation.

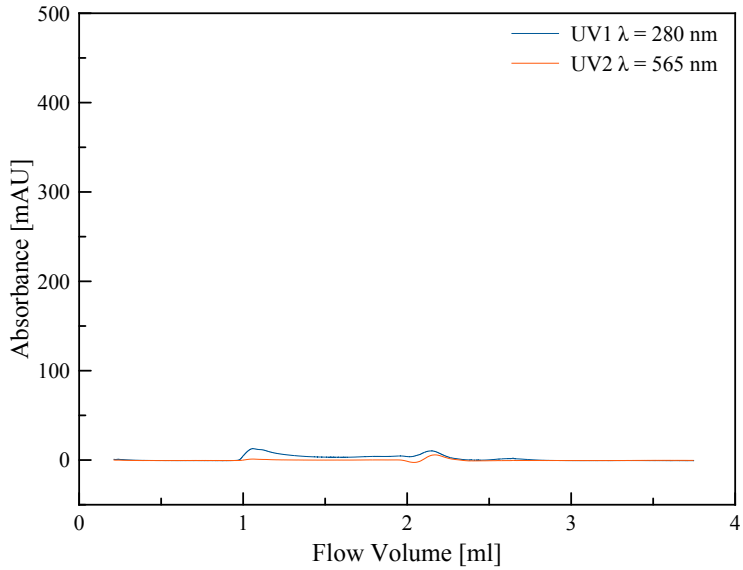

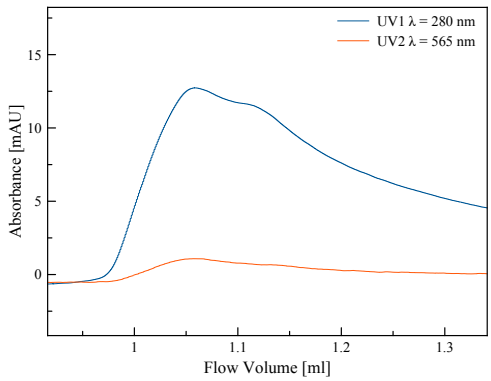

Figure 3.18 Elution profile second column. Liposome preparation in absence of dye. Whole profile and close-up to liposome peak. Both UV1 and UV2 show substantially lower amplitude as a consequence of the missing dye.

The liposomes diameter as analyzed by DLS was ~ 60 nm for the ones prepared by Rapid Dilution in presence of Sulforhodamine B and ~ 35 nm for those prepared in absence of dye.

To evaluate the encapsulation of Sulforhodamine B we utilized the fluorometric method. As presented in **Figure 3.19**, Rapid Dilution resulted in considerable dye encapsulation. **Figures 3.19A** and **B** show the fluorescence signal of a sample containing liposomes with encapsulated dye over time after the addition of detergent. It is evident, that the same amount of SDS liberates more dye than Triton X-100. To exclude that other reactions than the release and the dilution of the dye are responsible for the ~ 8-fold increase in fluorescence, we examined other possible causes:

- Liposomes without encapsulated Sulforhodamine B (**Figures 3.19C** and **D**) had been prepared via Rapid Dilution; Lipid Mix and Rapid Dilution Buffer did not contain the dye in that case. Addition of SDS only caused a moderate increase in fluorescence of 50%, while only a 15% increase was seen with Triton X-100.
- Fluorescence of a sample with Elution Buffer increased to not more than 1.75 of the basal value (**Figure 3.19E**).
- Finally we excluded interactions of the detergents with the dye directly by testing 50 mM Sulforhodamine B in Elution Buffer after addition of SDS (**Figure 3.19F**, 75% increase) and TritonX100 respectively (**Figure 3.19G**, 0% increase).

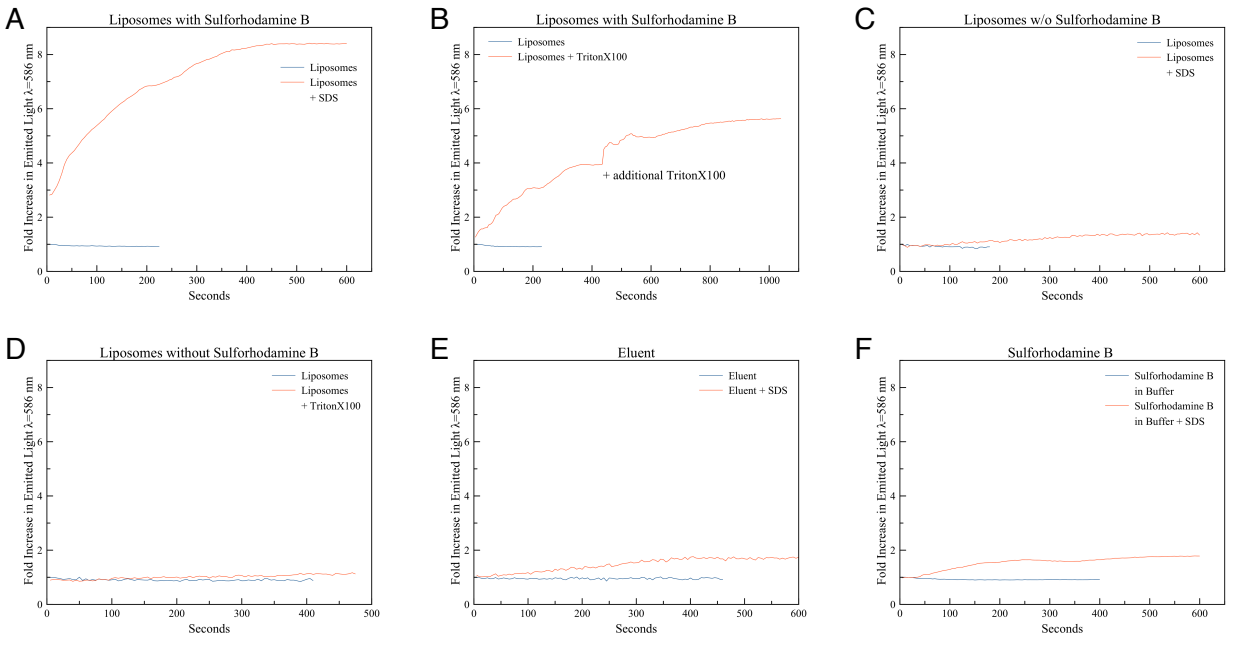

Figure 3.19 Liposomal dye encapsulation analysis via fluorometer. Prepared via Rapid Dilution method and purified via ÄKTApure. Blue lines represent basal fluorescence readings, red lines represent readings after addition of 0.1 V 20 % (w/w) detergent, freeing potential encapsulated dye. **A)** Liposomes with encapsulated Sulforhodamine B, addition of SDS. **B)** Liposomes with encapsulated Sulforhodamine B, addition of Triton X-100. Because of stalling of the reaction, another 0.1 V Triton X-100 were added to the sample. **C)** Liposomes prepared in absence of Sulforhodamine B, addition of SDS. **D)** Liposomes prepared in absence of Sulforhodamine B, addition of Triton X-100. **E)** Eluent response to SDS addition. **F)** 50 mM Sulforhodamine B in eluent, response to SDS addition. **G)** 50 mM Sulforhodamine B in eluent, reaction to Triton X-100 addition.

These results suggest that liposome preparation via Rapid Dilution leads to successful encapsulation of content dye. This encapsulation seems to favor larger liposomes (~ 35 nm without dye versus ~ 60 nm with dye at Rapid Dilution). However, liposome yield was poor and because of the time consuming preparation and our need for higher liposome concentrations we utilized another attempt.

Third Column

To optimize yield we utilized yet another column and adjusted the strategy by increasing the concentration of the Lipid Mix and by applying larger sample volumes to a Superdex™ 200 increase 5/150 GC.

Once again, the elution profile as recorded by the ÄKTApure shows sufficient separation of the liposomes from the excess dye (**Figure 3.20**). What seemed especially promising was once again the strong signal for Sulforhodamine B overlapping with the liposomes peak. The liposome-containing fractions furthermore had a distinct pink color that could be seen by eye. This suggests considerable encapsulation of dye.

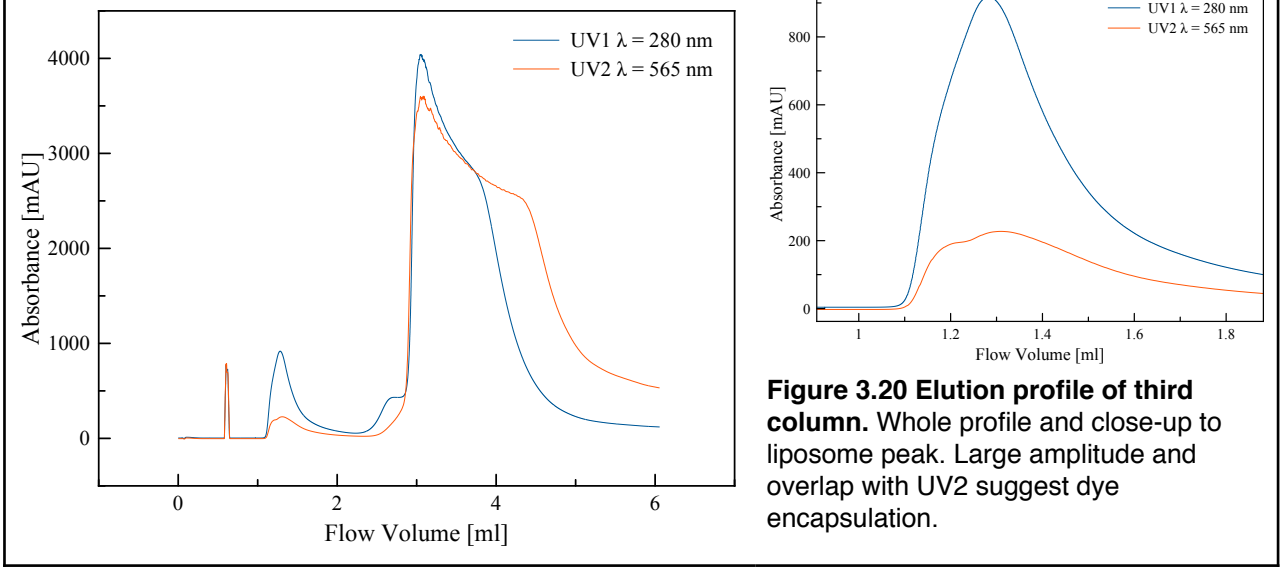

Figure 3.20 Elution profile of third column. Whole profile and close-up to liposome peak. Large amplitude and overlap with UV2 suggest dye encapsulation.

DLS measurements for these fractions revealed mostly liposomes with diameters of ~ 120 nm.

3.4. Liposomal attachment to spheroplast

The liposomal attachment to spheroplasts is the final, most critical step in the attachment assay and will also be decisive for the fusion assay. Thus we had to optimize conditions and the process until we got a reliable system.

3.4.1. Avidin addition to liposomes

The rationale behind the addition of the linking agent (streptavidin or avidin, respectively) to the biotinylated liposomes was to achieve a properly defined setup. Because of the experimental design there was no exact quantification of the biotinylation of spheroplasts. Inherent fluctuations in cell count and biotinylation efficiency rendered calculations of the appropriate amount of linking agent rather inaccurate.

The lipids of the Lipid Mix are solubilized by CHAPS and form liposomes when diluted below CMC, all in presence of Sulforhodamine B. This Rapid Dilution procedure typically forms ~ 65 nm large liposomes with encapsulated dye. Because of the high concentration of dye in both Lipid Mix and the diluting buffer, the dye is encapsulated at a self-quenching concentration.

Avidin or streptavidin can be added either directly after Rapid Dilution or after purification through gel filtration. Since the size exclusion limit of the first and second column is below the 60 kD for streptavidin, respectively 67 kD with avidin, which means that both linkers are not removed by these chromatography columns. They are consequently still present when the liposomes are added to the spheroplasts if no other steps are taken. Consequences and potential solutions are discussed in **4.6.**.

Initial attempts to evaluate liposome attachment event to spheroplasts consisted of spheroplasts incubating for extended periods of time in presence of liposomes at 4° C in the dark. **Figure 3.21** shows the results for a representative experiment done with this experimental outline. Prior to the experimental attachment phase spheroplasts had been biotinylated and (strept-)avidin

was introduced in the liposome preparation in 750-fold (avidin) or 420-fold excess (streptavidin) to the biotinylated lipid used in the lipid mix. The unnecessarily high excess was due to a miscalculation.

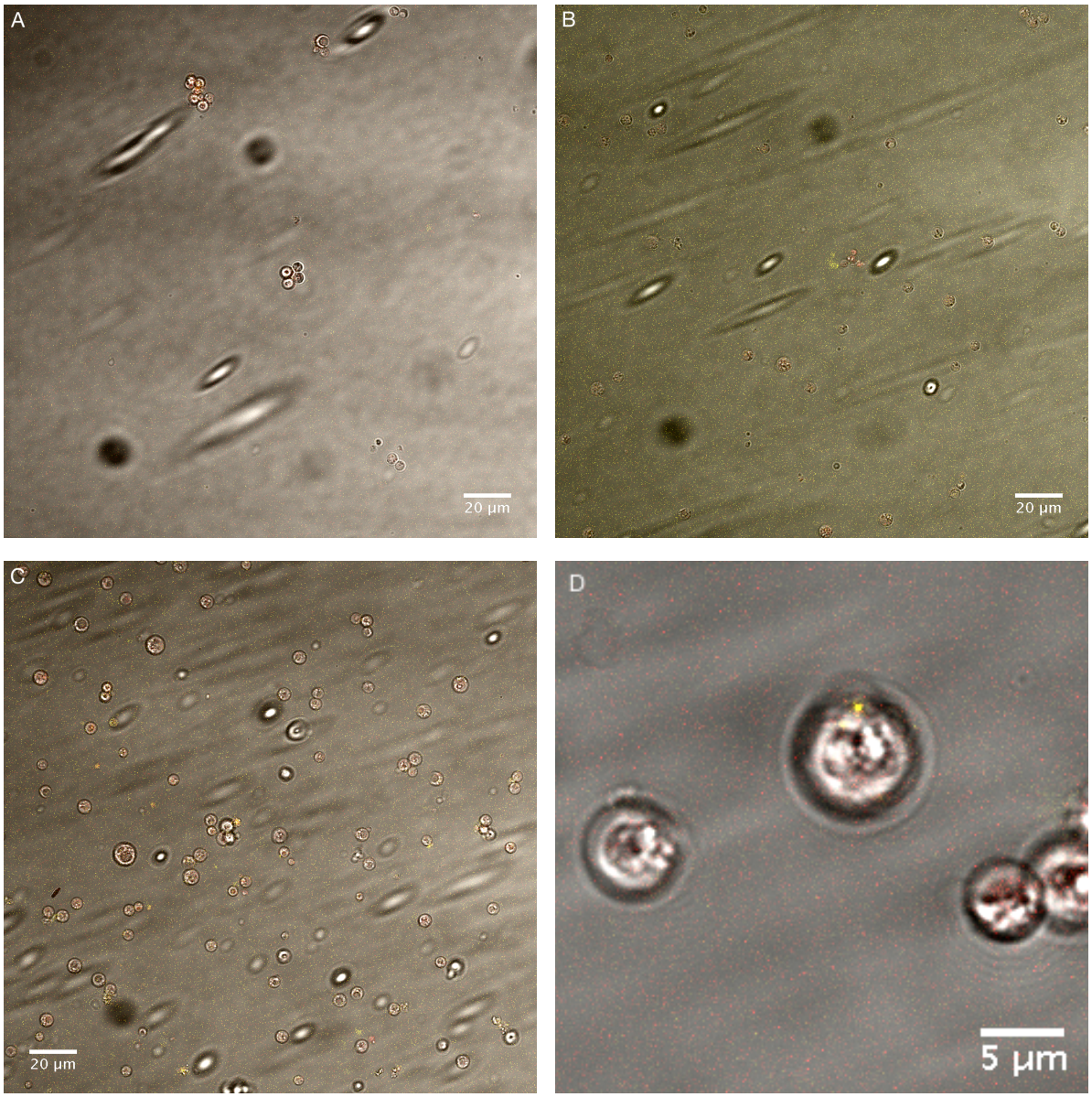

Figure 3.21 MATa **80 h after addition of liposomes and washing step. A)** Non-biotinylated spheroplasts with avidin-treated liposomes **B)** Biotinylated spheroplasts with avidin-treated liposomes. **C)** Biotinylated spheroplasts with streptavidin-treated liposomes. **D) Close-up of** biotinylated spheroplast with streptavidin-treated liposomes. The yellow spot is an attached liposome.

We concluded from these results that the excessive avidin or streptavidin, respectively, from the liposome preparation bound to spheroplasts. This would prevent liposomes to bind to spheroplasts in considerable amounts, because most biotins would be scavenged by free (strept-)avidin. Following this, a different approach was taken — the addition of linking agent to spheroplasts instead of liposomes.

3.4.2. Avidin addition to spheroplasts

Following the previous results, we decided to adjust our strategy: instead of adding the linking agent, such as avidin, to the liposomes, we decided to apply it to biotinylated spheroplasts. This change in our procedure had one central rationale: through multiple washing steps, we intended to remove most of the excessive avidin — hoping to prevent subsequently added liposomes from aggregation. As is demonstrated in **Figure 3.22**, we were not able to achieve this: both in the biotinylated and in the non-biotinylated sample there is abundant aggregation of liposomes. Because of the aggregates' size we were not able to remove them by centrifugation. During the investigation of attachment we found that regarding reaction kinetics a major part of the reaction should take place within 30 min at room temperature.

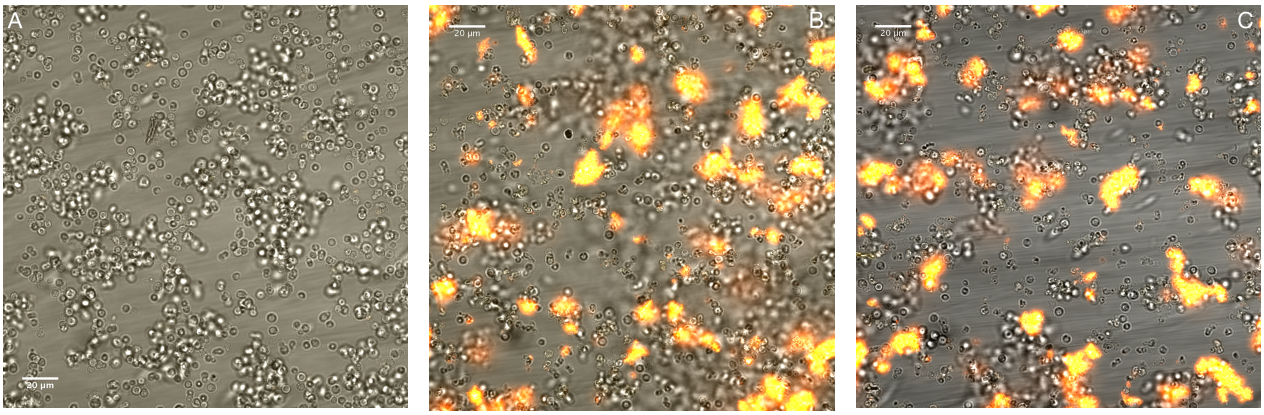

Figure 3.22 Attachment experiment with spheroplasts 30 min after addition of liposomes and two washing steps. Shown are overlays of transmitted light, Sulforhodamine B (red) and ATTO655 (yellow) fluorescence signal **A)** Non-biotinylated spheroplasts with liposomes in absence of avidin. **B)** Biotinylated spheroplasts, treated with avidin in advance. **C) Non-**biotinylated spheroplasts, treated with 5 mg/mL avidin in advance.

3.4.3. Concentration assessment

We traced the uncontrolled aggregation back to residual (strept-)avidin presence when we added the liposomes, leading to crosslinking. As a consequence we considerably reduced the concentration from 5 mg/mL of reaction volume too much lesser volumes, since the results in **Figure 3.14** were obtained with streptavidin concentrations of 25μg/mL and showed no obvious cross-linking between spheroplasts.

3.4.3.1. Comparison of streptavidin versus avidin

In parallel to the optimization of linker concentration, we analyzed the differences in specificity of streptavidin versus avidin. The summary of our findings is illustrated in **Figure 3.23**. 100 μL with ~ 3 x 10^7 biotinylated spheroplasts were treated with the indicated amount of (strept-)avidin for 30 min at room temperature (with occasional, gentle pipetting). After washing two times, the pellet was resuspended with 25 μL of liposomes as obtained from the ÄKTApure and diluted to 100 μL total volume using Spheroplasting Buffer. After another incubation period of 30 min at room temperature (again with sporadic,

careful mixing by pipetting), the spheroplasts were washed two times and resuspended in 150 μL of Spheroplasting Buffer and directly investigated under the microscope.

Our aim was to find a concentration of linking agent low enough that does not lead to unspecific reactions in the absence of biotin. At the same time it should be sufficient to enable attachment when spheroplasts are biotinylated.

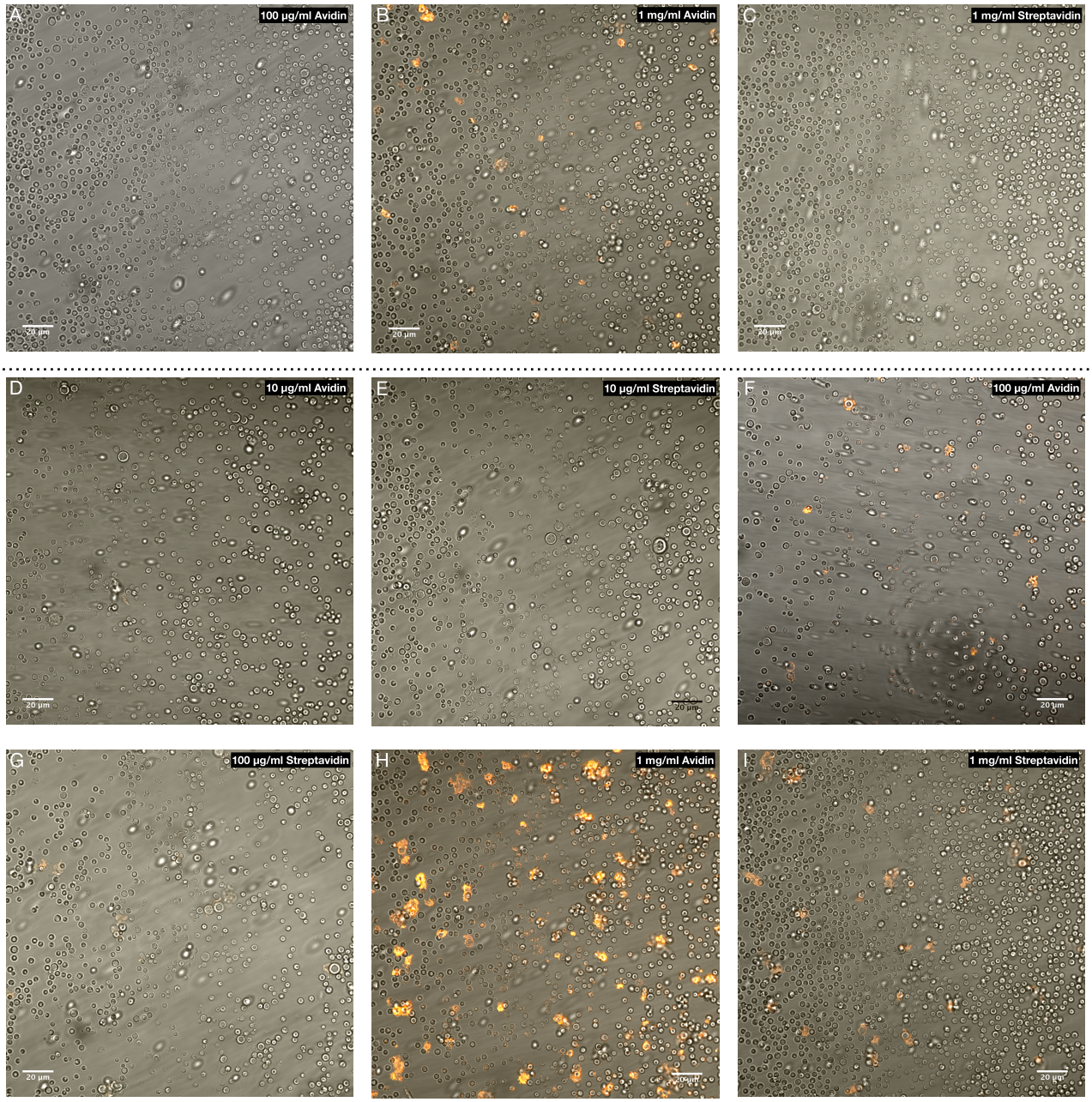

Figure 3.23 Assessment of optimal concentration for liposomal attachment of both avidin and streptavidin. A) Non-biotinylated spheroplasts with 100 μg/mL avidin, liposomes. **B) Non**-biotinylated spheroplasts with 1 mg/mL avidin, liposomes. **C) Non**-biotinylated spheroplasts with 1 mg/mL streptavidin, liposomes. **D)** Biotinylated spheroplasts with 10 μg/mL avidin, liposomes. **E)** Biotinylated spheroplasts with 10 μg/mL streptavidin, liposomes. **F)** Biotinylated spheroplasts with 100 μg/mL avidin, liposomes. **G)** Biotinylated spheroplasts with 100 μg/mL streptavidin, liposomes. **H)** Biotinylated spheroplasts with 1 mg/mL avidin, liposomes. **I)** Biotinylated spheroplasts with 1 mg/mL streptavidin, liposomes.

Figure 3.23A and **B** show such controls, with non-biotinylated spheroplasts and subsequent treatment with avidin and liposomes. In **A** with 100 μg/mL avidin applied there was no attachment detectable, but in **B** with 1 mg/mL avidin there was already considerable aggregation and occasional adhering to spheroplasts. In contrast to this finding it seems that 1 mg/mL of streptavidin did not lead to unspecific liposomal reactions (see **Figure 3.23C**).

When applied to biotinylated spheroplasts, 10 μg/mL of both avidin or streptavidin were not enough to promote attachment nor aggregation of liposomes (**Figure 3.23D** and **E**). Differences with the two could be observed when 100 μg/mL of either was used on biotinylated spheroplasts. In **F,** liposomes attached to spheroplasts that had been treated with avidin. Unfortunately, we also detected sparse aggregates. Addition to spheroplasts that had been treated with 100 μg/mL streptavidin yielded only liposomal enrichment at structures that appeared to be cell debris (**Figure 3.23G**).

1 mg/mL avidin treatment of biotinylated spheroplasts prior to addition of liposomes led to considerable attachment of liposomes to spheroplasts, but also to abundant aggregates (compare **Figure 3.23H**). Aggregates were not observed when biotinylated spheroplasts had been treated with 1 mg/mL streptavidin. However, even at this concentration streptavidin seemed to primarily target liposomes to cell debris (see **I**).

4. Discussion

4.1. MATa Δ*bar1* PRM1-GFP respond reproducibly to α-factor treatment

We have been able to show that MAT**a** Δ*bar1* PRM1-GFP responds in a reliable and reproducible manner to treatment with α-factor. The deletion in the *bar1* locus increases sensitivity to the pheromone by ~ 50-fold. A side-effect to this might be that abnormal changes in morphology, such as multiple shmoo formation, occurs when treated with α-factor for an extended period of time.

Polarization of Prm1-GFP in response to pheromone treatment in MAT**a** cells shows that the protein is enriched at the tip of the shmoo. We presume that this is also true for other fusion related proteins and the fusogen. Reduction in the polarization as well as decrease in the overall fluorescence over time suggest that the energy-demanding preparations for mating stress the cell. This would not happen during actual mating as the α-factor is subject to degradation by Bar1. Furthermore, a source of a sufficient amount of pheromone to elicit response must be in close proximity. Therefore the shmoo projection at the point of highest pheromone concentration should be able to establish contact and fusion can occur.

In contrast to exposure for an extended period of time, short exposure (up to three hours) to high concentrations of α-factor do not seem to have any adverse effect on MAT**a** cells. For our purposes it was sufficient to work with the lowest concentration that induces shmoo formation and Prm1-GFP expression.

4.2. Pheromone response of MATα is comparable to the one in MATa

Regarding the pheromone response of MATα, very few publications are available because of the difficulties in obtaining **a**-factor. We have been able to show that MATα is responsive to the synthetic **a**-factor, in contrast to a previous report [37]. This may be because of the higher quality of our synthesized **a**-factor or to the range of concentrations we examined: indeed, we have observed prominent shmoo formation after 3 h with 2.75 μg/mL and even more pronounced projections with 5 μg/mL as opposed to the 0.5 μg/mL used in the cited publication.

4.3. Spheroplasts are able to target Prm1 to the PM in a polarized manner

Results from our earlier spheroplasting experiments suggested that the procedure had adverse effects on the polarization of Prm1-GFP, even though the shmoo was well preserved. This has drawbacks for the experimental setup of the fusion assay as it relies on a high, localized concentration of fusion-related proteins to be retained at the PM. To remedy this unforeseen problem we investigated the pheromone response of spheroplasts directly. Indeed, in contrast to pheromone-treated cells that had been spheroplasted, spheroplasts that were pheromone-treated were able to express and target Prm1 to the PM in a polarized manner. The revision of our model is depicted schematically in **Figure 4.1**.

We also observed fluctuations of this polarization over the cell surface, as if searching for an anchor to stabilize polarization. Thus we propose that in an intact CW there is a molecule providing an anchor for the polarizing proteins at the forming shmoo tip.

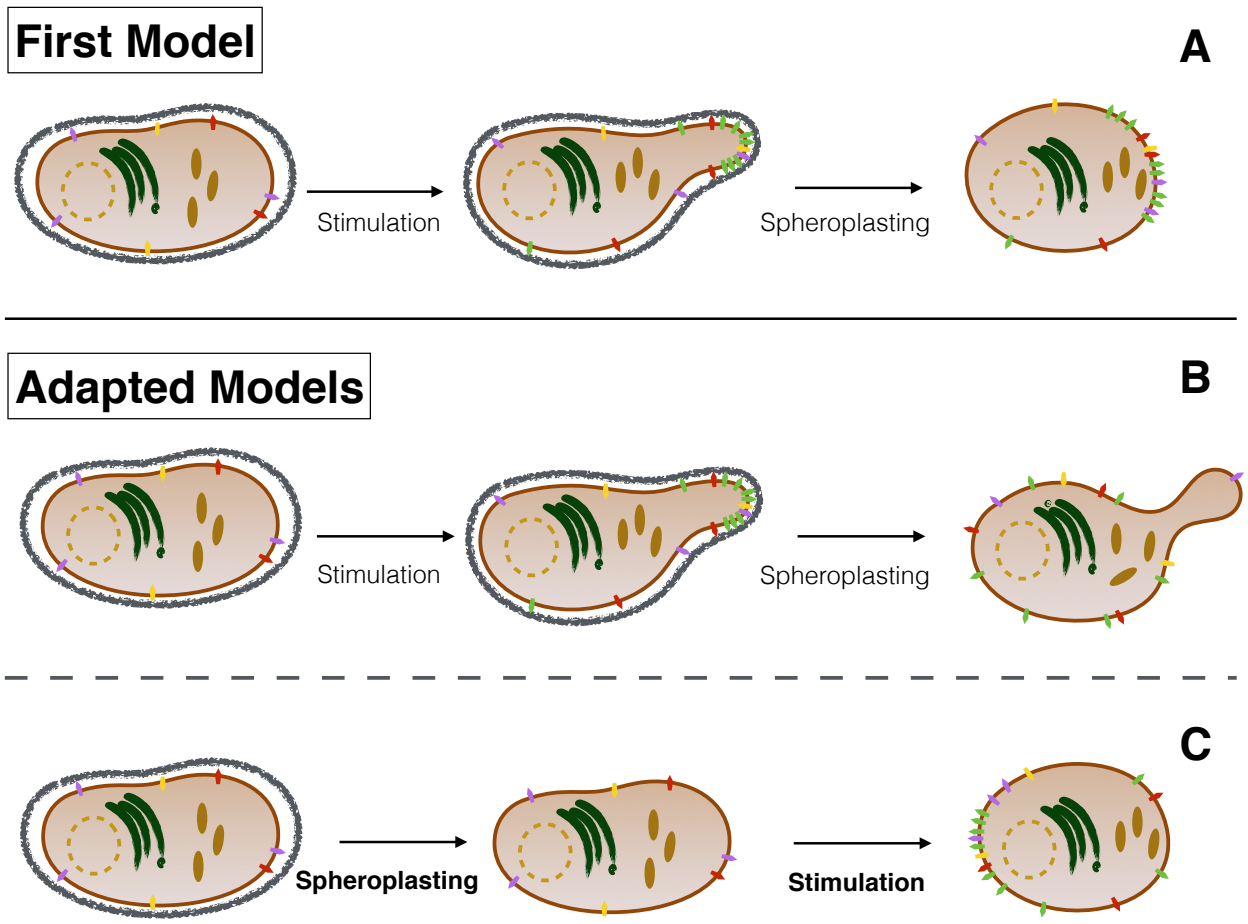

Figure 4.1 Hypotheses regarding spheroplasting and response to pheromone treatment. Comparison of first model and adapted models. **A)** First model shows how we expected stimulated cells would behave. **B)** Adapted model resulted from convergence of the hypothetical model to the experimental data. Note that once the CW is removed, the proteins disperse over the entire cell surface. **C)** Adapted model after reversing the order of the experimental setup. Spheroplasts are able to express and target Prm1 in a polarized manner as a response to pheromone treatment.

In order for the spheroplast to respond to pheromone treatment it needs a nutrient containing environment (such as in our case SC media). Two reasons are conceivable for this: it might either be because the response is energy demanding to an extent that the spheroplast is depleted from metabolic resources; or a starve signal pathway overrides the response through cell arrest.

We hypothesize that, just like Prm1, other proteins of the fusion machinery are targeted to the PM as well. Establishing polarization even in the absence of shmoo formation suggests that this mechanism is still intact, which is critical for the establishment of a functional Fusion Assay in the future.

4.4. Biotinylation does not adversely affect Prm1 polarization and vice versa

Once we showed that we can reliably biotinylate spheroplasts it was necessary to investigate whether biotinylation prior to pheromone treatment would affect the ability of the spheroplast to target Prm1 to the membrane. On the other hand it was necessary to examine whether pheromone treatment and the spheroplast's response would interfere with the biotinylation, e.g. via internalization of biotinylated PM proteins. Our analysis demonstrated that neither is the case. Samples with either biotinylation and/or pheromone treatment showed that treatment after biotinylation and found spheroplasts expressed and targeted Prm1.

Moreover it is noteworthy that the signal is not exactly superimposable. Although spheroplasts showed both Prm1 localization and biotinylation, the regions of highest Prm1 concentration were not associated with being more abundant in biotinylation.

4.5. Liposome preparation is a bottle neck

We investigated several methods for production of liposomes: directly in the column via gel filtration, via dialysis and Rapid Dilution and methods combining these apporaches. First diluting above the CMC via Rapid Dilution before dialyzing; dialysis with dye in the Dialysis Buffer; and preconditioning the gel filtration column with Rapid Dilution Buffer before injecting the Lipid Mix were among the strategies tested to yield liposomes in sufficiently large quantities for the assay. We were initially able to achieve this with most of the methods excluding dilution. However, Rapid Dilution was the only method that produced liposomes containing encapsulated dye as confirmed by fluorometric analysis. Unfortunately, the used method reduces the amount of lipids in the applied sample to 5 % of the original Lipid Mix. Moreover, subsequent purification via a gel filtration column dilutes the liposomes even further.

Interestingly, we found that the size of the liposomes varies with the method with which they were obtained. Generally speaking, liposomes via gel filtration were the smallest. Nevertheless, Rapid Dilution in the absence of dye resulted in liposomes of similar size suggesting that encapsulation of dye inherently leads to larger volumes. The liposomes via Rapid Dilution in presence of Sulforhodamine B were substantially larger, supporting this hypothesis. Approaches utilizing dialysis produced liposomes of > 100 nm in diameter. The pink color observed in the collected iposome fractions may be due to encapsulation at non-self-quenching concentration. To rule out possible methodological flaws, a complementary method to fluorometric measurements to assess dye encapsulation has to be considered.

4.6. Avidin/streptavidin can be used to attach liposomes to spheroplasts

Our results demonstrate the necessity biochemically attaching liposomes to spheroplasts since no spontaneous interactions were observed. For this purpose, avidin or streptavidin was added to biotinylated liposomes or biotinylated spheroplasts, but there are several points to consider. If (strept-)avidin is added to the liposomes, one can readily calculate the necessary excess (strept-)avidin to prevent undesired attachment between liposomes. This is much less straightforward in spheroplasts as concentration, spheroplasting and biotinylation efficiency vary for each experiment. As a consequence of the excess of (strept-)avidin there is no aggregation of

liposomes. The major drawback regarding this strategy though is that one cannot get rid of the unbound (strept-)avidin — even ultra centrifugation at 70 000 rpm was not able to sediment the liposomes.

Addition of avidin or streptavidin to biotinylated spheroplasts on the other hand presented different problems: although it should be possible to remove most of the unbound (strept-)avidin by centrifugation, it may be necessary to wash numerous times to achieve this. We found two washes to be insufficient when we applied 1 mg/mL avidin to biotinylated spheroplasts in the beginning. Still, despite the presence of aggregates we achieved considerably more attachment of liposomes. A possible solution might be to remove liposomes-aggregates with a low-rpm centrifugation: this way most of the spheroplasts should stay in solution while the aggregates sediment.

Thus it appears that the addition of streptavidin or avidin to the biotinylated spheroplasts is the method of choice for the Attachment Assay. Future work will have to determine optimal (strept-)avidin concentrations and the number of washing steps necessary to achieve the best signal/noise ratio without detrimentally affecting the spheroplasts. However, when future work will include reconstituted proteins in the liposomes, the method has to be reviewed again. As we have seen in preliminary experiments that were not included in the results chapter, proteoliposomes can be ultra centrifuged and thus excess (strept-)avidin can be removed. This possibility consequently renders this route much more attractive and could prove the method of choice with considerable attachment without liposomal aggregation.

Regarding the comparison of streptavidin and avidin, we cannot conclude at the moment which of those two linking agents serves our purposes the best. In theory, avidin should be less specific with binding than streptavidin, because of its glycosylation. Furthermore, it has been reported that avidin has an increased tendency to react with negatively charged PM and aggregate due to its basicity [43]. This could be a major factor in our issues of removal by washing. Whether the potentially more unspecific binding possesses problems to the actual attachment has yet to be determined — in our experiments we did not observe significant liposome attachment to non-biotinylated spheroplasts. Instead avidin showed a higher affinity towards biotin, as was suggested by previous studies [43, 44].

However, because of the abundant liposome aggregation we were not fully able to evaluate this. Once these difficulties are resolved, one should be able to thoroughly characterize the binding specificity of both streptavidin and avidin within this experimental setup.

4.7. Outlook

After the Attachment Assay is optimized by fine-tuning the use of (strept-)avidin, the next milestone will be to trigger fusion between liposomes and spheroplasts as a positive control. We did not observe spontaneous fusion in the experiments presented in this thesis, so future work will have to focus on ways to induce fusion of spheroplasts with attached liposomes. It is likely that this will be achievable by using polyethylene glycol (PEG) [45]. If Rapid Dilution is found to be *de facto* the only method to produce liposomes with encapsulated dye, it would be the method of choice despite the poor yields that can be achieved with it. Encapsulated dye at self-quenching concentration, the release of it into the cytoplasm and the subsequent increase in fluorescence will be crucial for assessment of fusion.

The pheromone response of spheroplasts provides new unanticipated opportunities for alternative experiments in search of the fusogen. One option would be to establish a pull-down

experiment using (strept-)avidin beads on biotinylatedspheroplasts. By comparing the pulled-down PM proteins (e.g. by mass spectrometry) before and after pheromone-treatment it should be possible to identify novel proteins with a fusion-related role.

Some results obtained in MAT**a** have to be confirmed in MATα, mainly pheromone treatment of spheroplasts.

Ongoing preliminary experiments suggest that it should not be too problematic to reconstitute proteins in liposomes using CHAPS. As mentioned above, this could even simplify some aspects regarding the attachment because of the possibility to use ultra centrifugation to wash and even concentrate proteoliposomes. The characterization and optimization of the proteoliposome protocol will be an essential step to test whether the basic fusion machinery in yeast can be reconstituted and fuse with the machinery present on the spheroplasts.

5. Literature

1. Klinovska, K., et al. (2014). "Sperm-Egg Fusion: A Molecular Enigma of Mammalian Reproduction." International Journal of Molecular Sciences **15**(6): 10652-10668.
2. Bromfield, E. G. and Nixon, B. (2013). "The function of chaperone proteins in the assemblage of protein complexes involved in gamete adhesion and fusion processes." Reproduction **145**(2): R31-42.
3. Aguilar, P. S., et al. (2013). "Genetic basis of cell-cell fusion mechanisms." Trends in Genetics **29**(7): 427-437.
4. Podbilewicz, B., et al. (2006). "The C-elegans developmental fusogen EFF-1 mediates homotypic fusion in heterologous cells and in vivo." Developmental Cell **11**(4): 471-481.
5. Chernomordik, L. V. and M. M. Kozlov (2003). "Protein-lipid interplay in fusion and fission of biological membranes." Annu Rev Biochem **72**: 175-207.
6. Chernomordik, L. V. and M. M. Kozlov (2008). "Mechanics of membrane fusion." Nature Structural & Molecular Biology **15**(7): 675-683.
7. Kobayashi, T., et al. (2002). "Separation and characterization of late endosomal membrane domains." Journal of Biological Chemistry **277**(35): 32157-32164.
8. Byrne, R. D., et al. (2007). "PLCgamma is enriched on poly-phosphoinositide-rich vesicles to control nuclear envelope assembly." Cell Signal **19**(5): 913-922.
9. Inoue, N., et al. (2005). "The immunoglobulin superfamily protein Izumo is required for sperm to fuse with eggs." Nature **434**(7030): 234-238.
10. Bianchi, E., et al. (2014). "Juno is the egg Izumo receptor and is essential for mammalian fertilization." Nature **508**(7497): 483-+.
11. Kaji, K., et al. (2000). "The gamete fusion process is defective in eggs of Cd9-deficient mice." Nature Genetics **24**(3): 279-282.
12. Takeda, Y., et al. (2003). "Tetraspanins CD9 and CD81 function to prevent the fusion of mononuclear phagocytes." Journal of Cell Biology **161**(5): 945-956.
13. Le Naour, F., et al. (2006). "Membrane microdomains and proteomics: Lessons from tetraspanin microdomains and comparison with lipid rafts." Proteomics **6**(24): 6447-6454.
14. Jegou, A., et al. (2011). "CD9 tetraspanin generates fusion competent sites on the egg membrane for mammalian fertilization." Proceedings of the National Academy of Sciences of the United States of America **108**(27): 10946-10951.
15. Runge, K. E., et al. (2007). "Oocyte CD9 is enriched on the microvillar membrane and required for normal microvillar shape and distribution." Developmental Biology **304**(1): 317-325.
16. Inoue, N., et al. (2011). "The mechanism of sperm-egg interaction and the involvement of IZUMO1 in fusion." Asian Journal of Andrology **13**(1): 81-87.
17. Rubinstein, E., et al. (2006). "Reduced fertility of female mice lacking CD81." Dev Biol **290**(2): 351-358.
18. Harrison, S. C. (2008). "Viral membrane fusion." Nature Structural & Molecular Biology **15**(7): 690-698.
19. Podbilewicz, B. (2014). "Virus and Cell Fusion Mechanisms." Annual Review of Cell and Developmental Biology, Vol 30 **30**: 111-139.

20. Bock, J. B., et al. (2001). "A genomic perspective on membrane compartment organization." Nature **409**(6822): 839-841.
21. Weber, T., et al. (1998). "SNAREpins: Minimal machinery for membrane fusion." Cell **92**(6): 759-772.
22. Lin, R. C. and R. H. Scheller (2000). "Mechanisms of synaptic vesicle exocytosis." Annual Review of Cell and Developmental Biology **16**: 19-49.
23. Podbilewicz, B. and J. G. White (1994). "Cell Fusions in the Developing Epithelia of C-Elegans." Developmental Biology **161**(2): 408-424.
24. Curto, M. A., et al. (2014). "Membrane Organization and Cell Fusion During Mating in Fission Yeast Requires Multipass Membrane Protein Prm1." Genetics **196**(4): 1059-1076.
25. Jahn, R., et al. (2003). "Membrane fusion." Cell **112**(4): 519-533.
26. Mewes, H. W., et al. (1997). "Overview of the yeast genome." Nature **387**(6632): 7-8.
27. Madhani, H. (2007). „From a to α. Yeast as a Model for Cellular Differentiation.“ Cold Spring Harbor Laboratory Press.
28. Olmo, V. N. and E. Grote (2010). "Prm1 Targeting to Contact Sites Enhances Fusion during Mating in Saccharomyces cerevisiae." Eukaryotic Cell **9**(10): 1538-1548.
29. Bardwell, L. (2004). "A walk-through of the yeast mating pheromone response pathway." Peptides **25**(9): 1465-1476.
30. Heiman, M. G. and P. Walter (2000). "Prm1p, a pheromone-regulated multispanning membrane protein, facilitates plasma membrane fusion during yeast mating." Journal of Cell Biology **151**(3): 719-730.
31. Aguilar, P. S., et al. (2007). "The plasma membrane proteins Prm1 and Fig1 ascertain fidelity of membrane fusion during yeast mating." Molecular Biology of the Cell **18**(2): 547-556.
32. Curto, M. A., et al. (2014). "Membrane Organization and Cell Fusion During Mating in Fission Yeast Requires Multipass Membrane Protein Prm1." Genetics **196**(4): 1059-1076.
33. Hallett, F. R., et al. (1991). "Vesicle Sizing - Number Distributions by Dynamic Light-Scattering." Biophysical Journal **59**(2): 357-362.
34. Pokorna, I. and A. Svoboda (1995). "Response of yeast protoplasts to their mating partners." Folia Microbiologica **40**(6): 583-587.
35. Vansolingen, P. and J. B. Vanderplaat (1977). "Fusion of Yeast Spheroplasts." Journal of Bacteriology **130**(2): 946-947.
36. Green, N. M. (1963). "Avidin.1. Use of [^{14}C]Biotin for Kinetic Studies and for Assay." Biochemical Journal **89**(3): 585-591.
37. O'reilly, N., et al. (2012). "Facile synthesis of budding yeast a-factor and its use to synchronize cells of a mating type." Yeast **29**(6): 233-240.
38. Mackay, V. and T. R. Manney (1974). "Mutations Affecting Sexual Conjugation and Related Processes in Saccharomyces-Cerevisiae. 1. Isolation and Phenotypic Characterization of Nonmating Mutants." Genetics **76**(2): 255-271.
39. Necas, O. (1971). "Cell Wall Synthesis in Yeast Protoplasts." Bacteriological Reviews **35**(2): 149-170.
40. Schirmer, E. C. and S. Lindquist (1998). "Purification and properties of Hsp104 from yeast." Molecular Chaperones **290**: 430-444.
41. Redd, M. J., et al. (1997). "A complex composed of Tup1 and Ssn6 represses transcription in vitro." Journal of Biological Chemistry **272**(17): 11193-11197.
42. Pobbati, A. V., et al. (2006). "N- to C-terminal SNARE complex assembly promotes rapid membrane fusion." Science **313**(5787): 673-676.

43. Wilchek, M. and E. A. Bayer (1988). "The Avidin Biotin Complex in Bioanalytical Applications." Analytical Biochemistry **171**(1): 1-32.
44. Kuo, T. C., et al. (2015). "Revisiting the streptavidin-biotin binding by using an aptamer and displacement isothermal calorimetry titration." Journal of Molecular Recognition **28**(2): 125-128.